

AD-A174 776

THE ROLE OF MODELING AND FLIGHT TESTING IN ROTORCRAFT  
PARAMETER IDENTIFICATION; NATIONAL AERONAUTICS AND  
SPACE ADMINISTRATION MOFFETT FIELD C.

R T CHEN ET AL

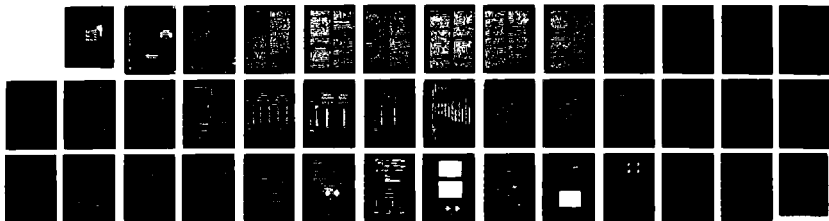
1/1

UNCLASSIFIED

JUN 86

P/G 1/3

NL



①

THE ROLE OF MODELING AND FLIGHT TESTING IN ROTORCRAFT  
PARAMETER IDENTIFICATION

by

R. T. N. Chen and M. B. Tischler

Ames Research Center  
Moffett Field, California

DTIC  
SELECTED  
DEC 02 1986  
S D

AD-A174 776

Presented at:

The 1986 AHS Forum, System Identification Session,  
Washington, D.C.  
June 2-4, 1986

**DISTRIBUTION STATEMENT A**

Approved for public release;  
Distribution Unlimited

DTIC FILE COPY

+

## THE ROLE OF MODELING AND FLIGHT TESTING IN ROTORCRAFT PARAMETER IDENTIFICATION

Robert T. N. Chen<sup>†</sup>  
NASA Ames Research Center, Moffett Field, CA

and

Mark B. Tischler<sup>\*</sup>  
Aeroflightdynamics Directorate, U.S. Army Aviation Research and Technology Activity  
Ames Research Center, Moffett Field, CA

### Abstract

The importance of recognizing that each lower-order model used for rotorcraft parameter identification has a limited range of applicability is illustrated in some detail. Examples are given to illustrate the use of conditioning the test input signals and the potential of using multi-axis test inputs to enhance the parameter identifiability. The paper discusses the benefits and limitations of using frequency sweeps as flight-test input signals for identification of frequency response for rotorcraft and for the subsequent fitting of parametric transfer-function models. This paper demonstrates the major role played by analytical modeling and the understanding of the physics involved in the rotorcraft flight dynamics, particularly understanding the limit of lower-order models, in achieving successful rotorcraft parameter identification.

### Notation

$a_0$  blade coning angle, rad  
 $a_1$  longitudinal first-harmonic flapping coefficient, rad  
 $a_2$  normal acceleration, ft/sec<sup>2</sup>  
 $A_{1c}$  lateral cyclic pitch, rad  
 $b_1$  lateral first-harmonic flapping coefficient, rad  
 $B_{1c}$  longitudinal cyclic pitch, rad  
 $F$  stability derivative matrix  
 $G$  control derivative matrix

$K$  gain  
 $L_i$  rolling moment derivatives  
 $N_i$  yawing moment derivatives  
 $p$  roll rate, rad/sec (or deg/sec)  
 $q$  pitch rate, rad/sec (or deg/sec)  
 $r$  yaw rate, rad/sec (or deg/sec)  
 $s$  Laplace transform variable, rad/sec  
 $T_i$  time constants, sec  
 $u$  longitudinal airspeed component, ft/sec  
 $\underline{u}$  control vector  
 $v$  lateral airspeed component (also inflow velocity), ft/sec  
 $V$  airspeed, ft/sec  
 $w$  vertical airspeed component, ft/sec  
 $x$  state vector  
 $Y_i$  side force derivatives  
 $Z_w$  quasi-static, vertical damping, 1/sec  
 $Z_{\theta_0}$  quasi-static collective effectiveness, ft/sec<sup>2</sup>/rad  
 $\theta$  pitch attitude, rad  
 $\phi$  roll attitude, rad  
 $\theta_t$  tail-rotor collective pitch rad  
 $\theta_0$  collective pitch, rad  
 $\delta_{LAT}$  lateral stick displacement (also,  $\delta_a$ ,  $\delta_{AS}$ ), in.

Presented at the 1986 AHS Forum, June 1986, Washington, DC.

<sup>†</sup>Aerospace Engineer. Member AHS.

<sup>\*</sup>Research Scientist. Member AHS.



Dist	Special
A-1	

es

$\delta_{rp}$	rudder pedals displacement, in.
$\delta_0$	collective stick displacement, in.
$\delta_r$	rudder actuator displacement, deg
$\delta_a$	aileron actuator displacement, deg
$\tau$	time delay, sec
$\sigma$	standard deviation
$\beta$	side slip (also flapping angle), rad (or deg)
$\omega_n$	undamped natural frequency, rad/sec
$\zeta$	damping ratio
$\lambda_i$	eigenvalues

### Introduction

For many years, research has been conducted by the helicopter industry and government agencies to develop global computer models such as C-81,<sup>1</sup> REXOR,<sup>2</sup> and CAMRAD,<sup>3</sup> which include comprehensive aerodynamics, structural dynamics, engines, and flight-control systems. For flight dynamics and control applications, the validity of these interdisciplinary, global computer codes can only be established by comparing their predicted responses with those actually measured in flight. Because of the numerous assumptions and approximations used and the large number of parameters involved in a global computer code, it is extremely difficult to fully establish its credibility by adjusting these assumptions and parameters to fit the measured data.

Simplified, special-purpose analytical models that are easier to operate and to comprehend can satisfy the needs in dealing with many aspects of flight-dynamic problems such as helicopter flying-qualities evaluation, design of stability and control augmentation systems (SCAS), and ground simulator validation. These simplified analytical models may be directly developed from the flight-test data by using modern system or parameter-identification techniques.

Significant advancement has been made in the field of aircraft state estimation and parameter identification in the last two decades. Two symposia<sup>4,5</sup> and an AGARD lecture series<sup>6</sup> have reviewed the state of technology in this field. These symposia and lecture series indicated that, while significant progress has been made in the identification of the stability and control

parameters of the fixed-wing aircraft, by comparison, progress has been relatively slow in its rotary-wing counterpart. Several important issues and problems are still facing rotorcraft parameter identification which need to be resolved if major advancements are to be achieved.

Unlike the flight dynamics of fixed-wing aircraft, rotary-wing aircraft's are characteristically those of a high-order system. Significant inter-axis couplings exist for single main-rotor helicopters<sup>7</sup>; dynamic interactions are present between the engine and drive train/rotor system<sup>8</sup>, and high-order effects such as rotor dynamics<sup>9-12</sup> and inflow dynamics<sup>13-18</sup> are inherently present in the system. The large number of degrees of freedom associated with the coupled high-order dynamics leads to a large number of unknown parameters that have to be identified, making it extremely difficult to achieve a successful application of system or parameter-identification techniques.

Special purpose lower-order models, valid for a limited range of frequencies or input-output magnitudes, may be used to reduce the number of unknown parameters to be identified. The selection of a lower order model is often dictated by its usage. For flight-control applications, for example, a model valid for a higher frequency range is required for the design and analysis of high bandwidth flight-control systems<sup>11-12</sup>; likewise, a model valid only for a lower frequency range such as one of quasi-static rigid-body dynamic models can be quite adequate for low bandwidth flight-control systems. Given a frequency range of interest, the determination of an appropriate dimensionality (or system order) for a lower-order helicopter model is not a simple task, however. Generally, in mathematics, the higher the order of a model, the better the fit to the observed input-output data over the range of frequencies of interest. What role, then, is to be played by physics and what by mathematics (or identification algorithms)? What type of a lower-order model should one use, parametric or nonparametric?

Whether a parametric or a nonparametric model is to be used for identification depends on the usage of the model and the identification procedure selected. For flight dynamics and control applications, parametric models such as state-space models or transfer-function models are preferred over nonparametric models such as impulse or frequency response. Identification of a parametric model can be conducted in either the time domain<sup>19-27</sup> or the frequency domain.<sup>28</sup> The latter can also be employed for identification of a nonparametric model first, then a parametric model.<sup>29-30</sup> Sophisticated software packages for both time- and frequency-domain system (or

parameter) identification have become commercially available in the past few years.<sup>31,32</sup> The key to a successful rotorcraft parameter identification may lie in the selection of appropriate lower-order models discussed above, and in the design of proper test inputs.<sup>33-35</sup>

The design of control input signals for flight testing is crucial for the identification of lower-order helicopter flight-dynamics models. Test inputs may be designed to optimize the information content in the helicopter response measurements within the frequency range of interest and, at the same time, minimize the excitation of the helicopter modes outside the frequency range of the model valid for its intended usage. Helicopter responses to a control input can be considerably nonlinear, especially in the vertical axis.<sup>18</sup> Care, therefore, must be exercised to devise the size of the test inputs so that the magnitude of the helicopter response is commensurate with the intended use of the identified model. To maximize the information content in the helicopter response data and thereby enhance the identifiability of the unknown parameters, especially those associated with interaxis coupling, it may be desirable to employ multi-axis, instead of single-axis, test inputs.

Other difficulties associated with rotorcraft parameter-identification include the relatively high noise level contamination in the response measurements, and the inherent instability of the basic aircraft. Means of overcoming some of these difficulties will be discussed in conjunction with the design of test inputs in the remainder of the paper.

#### Modeling Helicopter Dynamics for Parameter Identification

It is important to recognize that each analytical model used to fit the finite input-output data has a limited range of applicability. Recognizing this fact is of special importance in modeling helicopter dynamics for parameter identification, because a helicopter has a relatively large number of degrees of freedom. Awareness of the limitations of the analytical model is also of vital importance in the design of flight-test experiments, in processing the test data and selecting of parameter identification algorithms, and in correlation and interpretation of the identification results.

The selection of the range of applicability of the model is, of course, dictated by the motivation behind the identification. For example, if the model is to be used to validate a ground simulation involving large maneuvers, then the

appropriate candidate model would be nonlinear, not a linear model. If, on the other hand, the model is to be used for correlation with flying-qualities evaluation results or for flight-control system design involving possible use of high gains, then a better candidate would be a linear time-invariant model, not a nonlinear model. Two lower-order, linear, time-invariant models are now examined to illustrate their validity in terms of frequency range.

#### Validity and Limitation of a Quasi-Static Six-Degree-of-Freedom Rigid-Body Model

Consider a linear, time-invariant, nine DOF representation of the helicopter dynamics, which includes six DOF rigid-body dynamics and three DOF tip-path plane dynamics for flapping motion. This model is useful for the design of high bandwidth flight-control systems.<sup>10-11</sup> The model has the following form:

$$\begin{bmatrix} \dot{x}_R \\ \dot{x}_F \end{bmatrix} = \begin{bmatrix} F_{11} & F_{12} \\ - & - \\ F_{21} & F_{22} \end{bmatrix} \begin{bmatrix} x_R \\ x_F \end{bmatrix} + \begin{bmatrix} G_1 \\ G_2 \end{bmatrix} u \quad (1)$$

where  $x_R = (a_0 \ a_1 \ b_1; \dot{a}_0 \ \dot{a}_1 \ \dot{b}_1)'$ ,  $x_F = (\theta \ \phi \ q \ p \ r \ u \ v \ w)'$ , respectively, representing the state vector of the rotor and the body dynamics;  $u = (A_{1c} \ B_{1c} \ \theta_c \ \phi_c)'$  is the rotor control vector;  $F_{ij}$  and  $G_i$  are matrices of stability and control derivatives. Table 1(a) shows a set of numerical values of the stability and control derivatives of a representative teetering rotor helicopter in hover. The representation is a 10th-order system (the decoupled coning, yaw, and vertical degrees of freedom are not included).

A simplified six DOF model which assumes instantaneous response of the rotor may be developed from the nine DOF model (1) using the steady-state equation for the rotor dynamics. The resultant quasi-static six DOF rigid body dynamics model has the following form:

$$\dot{x}_F = (F_{22} - F_{21}F_{11}^{-1}F_{12})x_F + (G_2 - F_{21}F_{11}^{-1}G_1)u \quad (2)$$

The reduced lower-order model (6th-order) is shown in Table 1(b). The two low-frequency complex modes are the same for both models, but the real roots are more widely separated for the lower-order model. The differences between these two models are more clearly shown in their frequency responses.

A comparison of the frequency response of the fuselage pitch-and-roll rate to the lateral cyclic input for the 10th-order system and the 6th-order

system as given in Tables 1(a) and 1(b) are shown in Figs. 1 and 2. It is worth noting from these figures that, although the characteristic frequencies of the rotor dynamics and the body dynamics are well separated (by more than a factor of 10), the frequency range of applicability of the simplified 6th-order model is good only up to approximately twice that of the highest rigid-body characteristic frequency. In fact, if the amplitude ratio miss-match of a 6 dB or phase differential of 12° (whichever is more stringent), is used as the criterion, the maximum frequency that satisfies this criterion is approximately 2.5 r/s. Thus, it cannot be overemphasized that a simplified six DOF analytical model such as Eq. (2) has a limited frequency range of applicability.

To further demonstrate the point, consider two longitudinal cyclic inputs, one "doublet" with the dominant frequency content of approximately 1.57 r/s which is within the frequency range of applicability of the 6th-order model, and the other input with a dominant frequency content of 9 r/s which is beyond the frequency range of its applicability. Figures 3 and 4 show a comparison of the 6th- and 10th-order models using the two inputs mentioned above. These figures clearly indicate the importance of recognizing the frequency range of applicability of a simplified analytical model in designing and conditioning test inputs. Input design will be discussed later in the paper.

#### Limitation of Quasi-Static Vertical Dynamic Models in Hover

Now consider a linear time-invariant three DOF representation of the helicopter dynamics, which includes dynamic inflow, flapping, and the vertical motion of the helicopter<sup>18</sup> in hover. Again, this model may be useful for flight-control system design involving possible use of high gains in the vertical axis. A set of stability and control derivatives of an articulated rotor helicopter<sup>18</sup> for this 4th-order system is shown in Table 2. Following the procedure used to reduce Eq. (1) to Eq. (2), two reduced-order analytical models, one without inflow dynamics, and the other without inflow and flapping dynamics are calculated, with the results shown also in Table 2. These two reduced order models are represented by a 3rd-order and a 1st-order system, respectively, the latter being the conventional (quasi-static) vertical dynamics,

$$\dot{w} = Z_w w + Z_{\theta_0} \theta_0 \quad (3)$$

with  $Z_w = -0.304$  (1/sec), and  
 $Z_{\theta_0} = -293.34$  ft/s<sup>2</sup>/rad.

To provide some background for the results to be discussed in the subsequent sections, it is important to compare the calculated vertical-acceleration responses from the three models in Table 2 with that measured from flight using a CH-47B research aircraft.<sup>36</sup> Shown in Fig. 5 is a typical vertical acceleration response to collective step input with a magnitude of 0.62 in. (or 0.0201 rad collective pitch change). The data were taken initially with a sampling frequency of 107.75 Hz, then passed through a 5 Hz filter to remove the 3/rev (11 Hz) and higher harmonic vibratory noise. The filtered data were then decimated by a factor of 5 to yield 21.55 Hz data, as plotted in Fig. 5. As can be seen, the transient is characterized by an overshoot, which immediately follows the abrupt change in collective pitch. The response of the rotor RPM was not recorded, but some small variations in rotor RPM on the order of 3%, were observed from a video recording of the cockpit instrumentation during the flight. The response of the RPM is slower than that of normal acceleration, typically drooping down to its minimum at about 1 sec after an up collective, and the transient lasts for about 3 sec before reaching steady state.

The calculated perturbation of the vertical acceleration responses to a 0.62 in. step input in collective pitch is shown in Fig. 6 for the three models shown in Table 2. The 4th-order model, which includes dynamic inflow, flapping, and the vertical motion of the helicopter, matches the flight data reasonably well. The 3rd order model, which neglects the inflow dynamics, results in a degraded match with the flight data in the initial transient; and the quasi-static 1st-order model completely fails to capture the initial overshoot, which is a result of the combined effects of the two higher frequency modes, the inflow mode and the flapping mode.<sup>18</sup>

The validity, in terms of frequency range, of the two lower-order models can be seen more clearly by comparing their frequency responses with those of the 4th-order model as shown in Fig. 7. The calculations cover the frequency range of 0.1 to 100 rad/sec. A resonant peak at the frequency of about 17 rad/sec is evident from the 4th-order model. This is attributable to the destabilized flapping mode induced by the dynamic inflow<sup>18</sup> and can clearly be seen by comparing Fig. 7 (a) and (b). The frequency range of applicability of the 1st-order, quasi-static model is considerably lower compared to the 3rd-order model. If the criterion described previously for the six DOF rigid-body model is applied here, the frequency range of applicability is less than 5 r/s. The transfer functions of the vertical acceleration to the collective stick displacement are shown in Table 3. It is interesting to note

that both the 4th-order and the 3rd-order models exhibit nonminimum phase characteristics.

### Selection of Test Inputs

The test input is one of the most important factors affecting the accuracy with which model parameters can be identified. In fact, for a specified measurement system there is a theoretically achievable maximum parameter identification accuracy corresponding to each flight test input used to excite the helicopter. In the design of flight-test inputs, two important questions must be answered: (1) What should the input function be so that all the helicopter dynamic modes within the frequency range of interest are properly excited? (2) For how long should the data record be taken to enable identification of the parameters to a desired level of accuracy?

Many time-domain and frequency-domain approaches to the design of flight-test inputs for aircraft parameter identification have been extensively discussed in the literature.<sup>33,35</sup> These methods invariably involve maximization of some function of Fisher's information matrix or minimization of some function of the covariance matrix of the parameter-identification error. Since all the input-design procedures begin with a set of a priori values of the very parameters that are to be identified, no input-design procedure can truly be optimal in practice. For time-domain identification of aircraft stability and control parameters, some practical approaches to the design of "multi-step" test inputs have been developed using frequency analysis<sup>35</sup> or Walsh functions.<sup>34</sup> Figure 8 shows some typical multi-step input signals and their frequency distribution plots. For comparison purposes, a pulse input and a smooth test signal designed using the method of Ref. 33 are also shown in the figure. For the pulse or the multi-step input signals, there is considerably more power in the high-frequency region because of the sharp edges associated with these signals. Proper conditioning of these signals is, therefore, required if a successful identification of lower-order models is to be achieved.

### Conditioning of Input Signals

Because of the limited frequency range of applicability for lower-order models, proper design of flight-test inputs for identification of stability-and-control parameters of the helicopter is even more important. The highest frequency content of the flight-test inputs should be properly controlled so as to be consistent with the frequency range of applicability of the model. Otherwise, the results of parameter identification

would be very difficult to interpret and to correlate with those generated from a more complete model. Experience in applying the method outlined in Ref. 34 to a variety of aircraft has shown that the dominant frequencies contained in the test input signals are all lower than the highest characteristic frequency of the model, thus assuring the consistency of the input frequency distribution and the frequency range of applicability of the model. However, to insure that the high frequency content of these input signals does not exceed the frequency range of applicability of the model selected for parameter identification, a low-pass filter may be used to operate on the pilot input or on an automatic input device as schematically shown in Fig. 9.

The validity of this concept may be seen by comparing Fig. 10 with Fig. 4 as discussed in a preceding section. In Fig. 10, the high-frequency (9 r/s) doublet input applied in Fig. 4 was properly shaped using a 2nd-order filter with  $\omega_n = 2.5$  r/s and  $\zeta = 0.7$ . To achieve a better comparison, the amplitude of the doublet in Fig. 4 is increased so that the filtered input in Fig. 10 has the same peak amplitude as that in Fig. 4. Because of the attenuation of the high-frequency content of the input, a significant improvement is seen.

### Multi-axis Test Inputs

Multi-axis test inputs may be designed to enhance the identifiability of the helicopter unknown parameters, particularly those associated with the interaxis coupling. For example, the identification of the lateral-directional stability derivatives of a large fixed-wing cargo airplane may be considerably improved with test inputs involving simultaneous use of aileron and rudder. Shown in Table 4 are the separate aileron inputs and rudder inputs, both with a doublet and a pulse having their dominant frequency tuned to that of the Dutch-roll mode. For this particular example, the aileron inputs are much more effective than the rudder inputs in achieving smaller errors in identification of the lateral-directional stability derivatives. The aircraft responses to these inputs are not excessive and are on the same order of magnitude. Figures 11 and 12 show the aircraft responses to the rudder doublet and the aileron doublet, respectively.

The practical Walsh-function method of Ref. 34 was then used to design test inputs with simultaneous use of aileron and rudder. Two sets of "suboptimal" inputs are shown in Table 5. It is evident from Tables 4 and 5 that for the same data length of 16 sec, the suboptimal inputs provide better identification results than the conventional pulse and doublet inputs. Because of

the simultaneous use of both the aileron and the rudder, the suboptimal inputs also permit simultaneous identification of all the control derivatives in addition to all the stability derivatives. Thus, they are effective and economical. Figure 13 shows the aircraft responses to the suboptimal input II of Table 5.

For comparison purposes, an evaluation was also made for an alternate set of rudder and aileron inputs devised years ago by flight research engineers. This set of inputs can easily be performed by a test pilot by simply observing the bank angle. As shown in Table 6, a rudder step is first applied. When the bank angle reaches a prescribed value, say  $20^\circ$ , an aileron step is then applied to return the bank angle to  $0^\circ$ . At this point the rudder step is taken out, leaving in the aileron input. The aileron is later reversed to bring the bank angle back to  $0^\circ$ . As shown in Table 6, this set of practically implementable inputs by the pilot, though not as effective as the suboptimal inputs of Table 5, is significantly better than either the conventional aileron inputs or rudder inputs. Figure 14 shows the simulated aircraft response to this set of practical lateral-directional inputs.

Another practical input signal that has been used successfully in a number of rotorcraft flight tests<sup>29,30,39,40</sup> and nonrotorcraft flight tests<sup>37,38</sup> is the "frequency sweep." The frequency sweep provides good control over the frequency range of interest and so lends itself naturally to frequency-domain identification.

#### Frequency Sweeps

Two typical concatenated lateral stick ( $\delta_{LAT}$ ) frequency sweeps completed during the hover tests of a teetering rotor helicopter<sup>39</sup> are shown in Fig. 15. These tests used pilot-generated rather than computer-generated inputs. The sweep is initiated with two low-frequency sinusoidal shaped cycles, with the periods corresponding to the low-frequency bound of the desired identification range. For these particular tests, a nominal identification range of 0.4-15.0 rad/sec was desired, so the low-frequency period was  $T = 16$  sec. After the initial two low-frequency cycles, the control is moved at gradually increasing frequency for another 50 sec. By the end of the run, the control is being driven quite rapidly (about 4 Hz in Fig. 15) with generally smaller displacements. The control is then returned to trim, ending the approximately 90 sec test period. At least two repeat sweeps are performed consecutively for each control to ensure a sufficient amount of dynamic data for the identification process.

The input autospectrum ( $G_{\delta\delta}(\omega)$ ) in Fig. 16 displays the frequency distribution of the concatenated excitation signal ( $\delta_{LAT}$  of Fig. 15). The frequency-sweep produces nearly constant power in the range of 0.3-7.0 rad/sec. The spectral content apparent below the minimum average input frequency of  $\omega = 0.4$  rad/sec ( $T = 16$  sec) results from the various nonsinusoidal low-frequency input signal details. At high frequency ( $\omega > 7$  rad/sec), the reduced autospectrum reflects the deliberate reduction in input amplitude (this is also apparent in Fig. 15) which was necessary to avoid overly exciting the rotor-pylon dynamics. The pilots could comfortably generate sizable inputs up to a frequency of about 4 Hz.

The frequency-sweep input is especially well suited for frequency-domain identification procedures because:

- (1) The input autospectrum is generally constant over the desired frequency range.
- (2) The wave form is roughly symmetric, so the mean and linear drift can be extracted by noniterative algebraic means--a requirement for nonparametric identification.
- (3) The input and output wave forms are smooth and regular, so the resulting spectral functions are well behaved. (Multi-step inputs, if not conditioned properly, are not suitable for frequency-domain identification because the abrupt wave form generates undesirable side-lobes in the spectral functions.)
- (4) The frequency buildup is slow and steady (as seen in Fig. 15) which allows the sweep to be terminated if structural mode excitation is encountered. Multi-step inputs may "ring" the aircraft natural modes simultaneously unless conditioning is used.

Some problems encountered with frequency-sweep testing are:

- (1) The long testing run needed to identify low-frequency dynamics generally requires that the hover tests be conducted with the stability augmentation system engaged. Thus, the extraction of open-loop dynamics is sensitive to correlation of the excitation signal (e.g., surface deflection) with the feedback signal. Success in extracting open-loop dynamics from closed-loop testing is essentially a signal-to-noise problem that can be overcome if the feedback gains are not very high.<sup>30</sup>
- (2) For highly coupled (e.g., single-rotor) helicopters, off-axis excitation is unavoidable and must be regulated by some movement of the "nonswept" controls. (This difficulty is

particularly noticeable in the hover condition.) Such secondary regulation is acceptable and can be accounted for in the analysis if the swept and nonswept inputs are not fully correlated.<sup>19,30</sup>

(3) As seen in Fig. 15, the pilot's input amplitude changes as a function of frequency. In hover, for example, large low-frequency inputs are not possible. High-frequency input amplitudes are also often reduced because rotor or structural resonances and actuator authority limits are encountered. Thus, nonlinear characteristics may not be exposed consistently across the frequency range, or from one repeat run to the next. In general, these inconsistencies are considered acceptable since the pilot's input amplitude during the frequency sweeps is representative of his normal operating control technique. The resulting models are describing-functions which reflect the "average" dynamics of the rotorcraft in its normal operating envelope.

While the sweep can be computer-generated (as in Ref. 40), pilot-generated inputs have some important advantages:

(1) Since pilot test technique differs somewhat in each repeat run, the concatenated records generally contain good spectral content over the entire frequency range of interest. The differing input amplitudes for each run yield a model which reflects the average vehicle dynamics over a wide operating range of amplitude and input forms.

(2) Although computer-generated sweep inputs are symmetric, the responses will not be symmetric and can cause the aircraft to drift significantly away from the reference trim condition. This behavior is apparent in the computer-generated sweeps of Ref. 40. When the pilot generates the sweep input, low-frequency trim inputs can be used to correct the drifts in the reference condition.

(3) Finally, the manual sweeps give the pilot full control over the conduct of the tests and the magnitudes of the inputs which is a particular concern in hovering tests.

Some useful guidelines were compiled by the pilots who executed the frequency-sweep tests on the teetering rotor helicopter.<sup>39</sup> They are given in the Appendix.

#### Rotorcraft-Parameter Identification

Dynamics identification methodologies generally fall into two categories: frequency-domain and time-domain. Each approach has its inherent strengths and weaknesses which make it best suited for particular applications. Time-domain (maximum likelihood) identification (Fig. 17) uses Kalman-

filter technology to obtain unbiased estimates of state-space model parameters. Such a model facilitates a direct comparison between stability derivatives obtained in the wind tunnel and those of the actual flight vehicle. Transfer functions and frequency responses are by-products of time-domain identification since they are calculated from the extracted state-space model but are not identified explicitly. Thus, models which provide a good fit in the time-domain do not necessarily yield transfer functions that accurately reflect the frequency-domain behavior. One reason for this is that time-domain identification uses least-squares fitting along a linear time scale, while transfer functions and frequency responses are displayed on a logarithmic scale of frequency. Therefore, time-domain identification techniques weight their results more heavily at low frequency where the majority of the data points are concentrated.

While time-domain identification methods have been extensively applied to fixed-wing vehicles, similar experience with rotorcraft is limited. In the Federal Republic of Germany, the German Aerospace Research Establishment (DFVLR) has conducted extensive studies in parameter identification of rotorcraft dynamics using maximum likelihood time-domain techniques. Much of this research has been associated with the highly coupled BO-105 hingeless rotor helicopter.<sup>20,21</sup> In the National Research Council of Canada, a time-domain, quasi-linear response-error method was used for identification of helicopter stability and control derivatives.<sup>24</sup> Recent work in time-domain identification of rotorcraft has also been reported by researchers at the Royal Aircraft Establishment (RAE), Bedford, England.<sup>27</sup>

The frequency-domain-identification approach depicted in Fig. 18 uses spectral methods to extract the frequency responses between selected input and output pairs. The identification results are presented in Bode-plot format: magnitude and phase versus frequency. These nonparametric identification results are very useful for flight-control system design and handling qualities studies. Currently proposed handling-qualities criteria for the LHX (Ref. 41) are based on frequency-domain parameters which can be read directly from these graphical results. Frequency responses obtained from real time and nonreal time simulations can be compared directly with the flight data to expose limitations and discrepancies in the simulator models. The fact that this comparison can be made without an a priori assumption of model structure or order is especially important for verifying mathematical models of new aircraft configurations. Tabulated frequency responses are fitted with analytical transfer-function models to extract modal characteristics

which are useful for handling-quality specifications given in lower-order equivalent system terms and for transfer function-based control system design studies. Since this fitting procedure is completed after the frequency response is extracted, the order of the transfer function can be carefully selected to avoid an overparameterized model. Multi-input/multi-output frequency-response methods are suitable for extracting a transfer matrix which includes the important coupling effects.<sup>30</sup>

Once the transfer functions are identified, state-space models given in terms of modal or canonical coordinates can be realized. State-space models can also be extracted in terms of the physical state variables using least squares fitting of the transfer-function parameters or frequency responses.<sup>28</sup> Finally, the extracted models are driven with the flight data to verify the time-domain characteristics. The semilog frequency format of the Bode-plot presentation and subsequent transfer-function fit makes the identified transfer-function and state-space models most accurate at mid and high frequency (initial time history transients). The low-frequency and steady-state response prediction of the extracted models is generally not as good as in the time-domain identification approach.

While frequency-domain identification of fixed-wing aircraft has been conducted for many years, its application to rotorcraft identification is fairly recent:

1. XV-15 tilt rotor aircraft.<sup>29,30</sup>
2. Bell-214-ST.<sup>39</sup>
3. NASA/Army CH-47B.<sup>18</sup>
4. Canadian NRC-205.<sup>40</sup>

The first three aircraft are being investigated by the authors and are discussed in the following sections.

#### Frequency-Domain Identification of the XV-15

The frequency-domain identification of the XV-15 tilt-rotor aircraft (Fig. 19) is an extensive on-going research effort. The objectives of this project, begun in 1983, are to identify and document the open-loop dynamics of the XV-15 throughout its flight envelope, to compare the simulation and flight responses, and to develop and verify a transfer-function model description for future use in control-system development. Identification methodologies, computational techniques, and discussion of results are covered in detail in Refs. 29 and 30. Included in this research have been multi-input/multi-output

identification, multi-axis transfer-function fitting, and structural-dynamics identification. The current work involves the comparison of frequency-domain and time-domain identification results for the hover condition.

#### Identification of Lower-Order Equivalent Transfer Functions of Bell 214-ST

Frequency-domain testing of the Bell 214-ST single-rotor helicopter (Fig. 20) was completed in October 1985 in support of the Army's development of an updated Mil-H-8501 and LHX handling-qualities specification.<sup>41</sup> These tests were intended to demonstrate the frequency-domain identification procedure on a single-rotor helicopter since much of the previous methodology development had been completed on the (twin-rotor) XV-15 aircraft. A discussion of the testing procedures and identification results for the Bell-214-ST is presented in Ref. 39. This project showed the feasibility of frequency-sweep testing and frequency-domain identification for use in helicopter handling-qualities specifications. Further, the results showed that very low order transfer-function models can accurately predict the large motion time-domain behavior of helicopters--even in hover. An example of the results excerpted from the report on the Bell-214-ST test<sup>39</sup> is given below to illustrate the frequency-domain identification approach.

The lateral stick frequency-sweep input and the corresponding input auto spectrum for the hover-flight condition (with the control system engaged) was previously presented in Figs. 15 and 16. The associated roll rate response for these two frequency sweeps is shown in Fig. 21. The maximum roll rate is about  $\pm 15^\circ$  per sec, with somewhat lower values for very low and very high frequency inputs. The corresponding output auto spectrum (Fig. 22) shows that the roll rate excitation is roughly constant in the frequency range of 0.3 to 7.0 rad/sec, which corresponds to the frequency range over which the input auto spectrum is constant (Fig. 16). At high frequency, the spectral response drops off owing to the K/s response roll-off of the rigid body helicopter dynamics and to the reduced pilot inputs at high frequencies (Fig. 15). The peak which occurs at  $\omega = 11.9$  rad/sec is due to the excitation of the rotor-pylon structural mode. The output auto spectrum drops sharply for frequencies below 0.1 rad/sec since there is very little pilot input at these low frequencies.

The frequency response of roll rate to lateral stick ( $p/\delta_{LAT}$ ) is shown in Fig. 23. At the higher frequencies considered, the response exhibits a K/s characteristic which indicates that a constant roll acceleration results from an initial

input of lateral stick. The presence of the rotor-pylon mode at  $\omega = 11.9$  rad/sec is clearly seen in the figure. At very low frequencies, the roll rate is reduced significantly because of the large lateral velocity perturbations.

The quality of the identified frequency response can be assessed from the coherence function shown in Fig. 24. This frequency-dependent parameter may be interpreted as that fraction of the output spectrum estimate which can be accounted for by linear relation with the input spectrum estimate. Thus, when the process under investigation is perfectly linear and the spectral estimates are noise free, the coherence function will be unity for all frequencies in the excited input spectrum range. A value of the coherence function less than unity will result from nonlinearities in the system, input/output noise, or cross-coupled control inputs. As can be noted in Fig. 24, good frequency-response identification is achieved in the range of 0.2 to 12.0 rad/sec. The oscillation in the coherence function for frequencies greater than 12.0 rad/sec and the rapid decline in coherence function for frequencies below 0.3 rad/sec are strong indications of reduced spectral estimate accuracy. The identification at low frequency can be improved by reducing the period of the first two frequency sweep cycles (Fig. 15). High-frequency excitation for the Bell-214-ST tests was restricted because of the excitation of the rotor pylon mode.

The next step in the identification procedure is the fitting of lower-order transfer-function models. In the case of the XV-15 study, the open-loop coupled dynamics were sought. Therefore, the selected model orders corresponded to the physical order of the coupled open-loop dynamics.<sup>30</sup> This is consistent with the earlier discussion on model order selection in the present paper. In the Bell-214-ST study, closed-loop transfer-function models were sought. The overall effect of the closed-loop augmentation is to drive the open-loop poles into the zeros, thereby suppressing the open-loop inter-axis coupling and reducing the residues of some of the open-loop modes. An appropriate closed-loop representation for the purposes of this study was one that accurately modeled the dominant on-axis closed-loop responses and ignored the off-axis responses and nearly canceled modes. Therefore, the transfer-function order was selected as a minimum order which would yield a reasonable fit of the flight data. In the case of the roll (and pitch) closed-loop attitude dynamics of the Bell-214-ST, the following second-order transfer-function form was found to adequately reflect the dynamics of the helicopter both in hover and cruise:

$$\frac{p}{\delta_{LAT}}(s) = \frac{Ks e^{-\tau s}}{(s + 1/T_1)(s + 1/T_2)} \quad (4)$$

The exponential term in the numerator is included to account for the phase lag due to high-frequency dynamics such as the rotor and actuators.

The maximum frequency range usable for transfer-function fitting corresponds to the region of maximum coherence (0.2-12.0 rad/sec) in Fig. 24. However, the 2nd-order model of Eq. (4) only accounts for the rigid body dynamics, so the fit must be restricted to the frequency range which excludes the rotor-pylon resonance. Thus, the "frequency range of model applicability" is 0.2 to 10.0 rad/sec. This approach is consistent with the earlier discussion of vertical acceleration models.

Applying the transfer-function form of Eq. (4) to fit the roll rate response of Fig. 23 in the range of 0.2 to 10.0 rad/sec yields the following numerical parameters:

$$\left. \begin{aligned} K &= 35.41 \text{ deg/sec}^2/\text{in.} \\ \tau &= 0.050 \text{ sec} \\ \frac{1}{T_1} &= 0.38 \text{ rad/sec} \\ \frac{1}{T_2} &= 2.83 \text{ rad/sec} \end{aligned} \right\} \quad (5)$$

Referring to Eq. (5), it can readily be seen that the roll response is heavily damped (no complex-valued roots) with a dominant response time constant of  $T_2 \approx 0.3$  sec. The small effective time delay of  $\tau = 0.050$  sec shows that the rotor, actuator, and structural dynamics do not cause significant phase lag in the frequency range of concern for piloted handling qualities (about 0.1 to 10.0 rad/sec). As shown in Fig. 23, the extracted model fits the data very well in the frequency range of applicability (0.2-10 rad/sec).

The ability of this simple transfer-function model to predict the time-domain roll response characteristics in hover was tested using aircraft response to step inputs. This input was selected for the verification study to show the robustness of the extracted model in predicting response characteristics to input forms other than the frequency-sweep form used in the identification process. However, as discussed earlier, the step input has high-frequency spectral content which excites aircraft modes outside of the transfer-function model's range of applicability (0.2-10.0 rad/sec). Most important is the unwanted excitation of the rotor-pylon resonance

( $\omega = 11.9$  rad/sec). Therefore, the input and output flight data are low-pass filtered to attenuate the spectral content for frequencies beyond  $\omega = 10.0$  rad/sec. The filtered step input flight data are used to drive the transfer-function model for comparison with the filtered output flight data. These filtered time histories are shown in Fig. 25.

A fairly large step input of  $\delta_{LAT} = 0.75$  in. was applied and held constant until a maximum steady-state roll rate was achieved (about  $7^\circ/\text{sec}$  as seen in Fig. 25). The transfer-function model is seen to closely reflect the filtered roll rate response over the entire time history including the recovery phase. The differences which are apparent in the regions of maximum roll rate mostly result from using a single-axis model (Eq. (4)), which ignores the contribution of the off-axis inputs. The very good overall match between the flight data and the transfer-function model response shows the utility of this fairly low-order model in characterizing the closed-loop dynamics of the Bell-214-ST. The fact that the prediction is very good for this (smoothed) step input form, which is markedly different in shape from the frequency sweep, shows the robustness of this identification approach and the advantage of using minimum-order transfer-function models.

#### Identification of CH-47B Vertical Dynamics Model in Hover

The same frequency-domain procedure used in the identification of the two preceding aircraft was also applied to the identification of the vertical dynamics of the CH-47B research aircraft (Fig. 26) in hover. A varying frequency input in collective pitch was employed to identify first the frequency response of the vertical acceleration to collective input. Figure 27 shows a sample of typical frequency sweeps of the input with frequency varying from about 0.05 Hz to about 2 Hz. The normal acceleration response with a discernible lead in low frequency is also shown in the figure. Because of some sharp edges in the frequency sweeps, substantial power in the collective input beyond 2 Hz (slightly above 3 Hz) is present, as can be seen in the input auto-spectrum and input-output cross-spectrum plots shown in Fig. 28.

The extracted frequency response as shown in Fig. 29 and the accompanying coherency function (Fig. 30) indicate that the nonparametric identification is good between the frequency range of 0.2 to 20 r/s. The transfer-function amplitude plot shows that there is a resonant peak at around 17 r/s as predicted earlier in Fig. 7. The predicted phase lead in the low-frequency region

shown in Fig. 7 also appears in the identified transfer-function phase plot in Fig. 29.

Guided by the analytical modeling efforts discussed in the previous section, a series of parametric transfer-function models, ranging from 1st to 5th order was fit to the identified frequency-response plots. The results which are listed in Table 7 are classified according to the order of the denominator. The 1st-order model corresponds to the quasi-static model shown in Table 3. The next higher-order model selected for fitting the frequency-response plots is a 3rd-order model which corresponds to the no dynamic-inflow case (Case (b) in Table 3); no 2nd-order models were used. Two 4th-order models were used: one with 4th order in numerator (which corresponds to Case (a) in Table 3) and the other with 3rd order in the numerator (which corresponds to the case having no direct control effective on the vertical acceleration due to blade pitch changes).<sup>18</sup> The 5th-order model was used to account for possible effects due to variation in rotor RPM.

The frequency-response fits for a 1st- and a 4th-order model (models (a) and (e) in Table 7) are shown in Fig. 31. For the 1st-order model, it proved to be difficult to fit the model accurately over the entire frequency range; the fit was, therefore, limited to the range of 0.1 to 3 r/s, instead of 0.1 to 20 r/s as applied to all other models. This causes the 1st-order model to match the flight data better at low frequency than the higher-order models, as can be seen in Fig. 31. All the higher-order models exhibit a nonminimum phase characteristic as predicted in the analytical modeling previously shown in Table 3. The index for the fitting error improves as the order of the transfer-function numerator and denominator increases because of more free parameters available for fitting the data. It is noted in Ref. 42, however, that a model with more free parameters, though in general achieving a better fit to a set of given data, does not necessarily provide a better predictive capability (which, after all, is the very purpose of developing a model).

As a means for testing the predictive capability of those six identified models, the vertical-acceleration responses to a step input in collective input (0.62 in.) were generated from the models. (In calculating these responses, the small time delay (or advance) contained in the models was neglected.) These responses of the identified models (Fig. 32) compare very favorably with those of the analytical model (Fig. 6). The responses of the two identified 1st-order models (a and b), a 4th-order model (e), and the 5th-order model (f) are plotted together with flight

data (of Fig. 5) in Fig. 33. As expected, the 1st-order model (a), because of its limited frequency range of applicability, fails completely to predict the overshoot of the vertical acceleration owing to the high-order effects of inflow and flapping dynamics. However, the long-term response matches well with the flight data. The other identified 1st-order model (model (b)), which fits over the entire frequency range with a large fitting error, produces a response that attempts to compromise the initial and final responses of the flight data. As a result, its response is inconsistent with the responses of other models and its range of applicability and usefulness becomes rather uncertain. The 4th-order model provides a much better predictive capability than does the 1st-order ones for the initial transient. The response of the 5th-order model matches even better with the flight data in the initial transient, but its long-term response becomes somewhat worse than that of the 4th-order model, indicating that overparameterization may be present in the 5th-order model.

#### Concluding Remarks

This paper has discussed in some detail the importance of recognizing that each lower-order model used for rotorcraft-parameter identification has a limited range of applicability. Awareness of this fundamental limitation is of paramount importance in designing flight-test experiments, in processing the test data, and in interpreting the identification results. Test-input signals must not only be designed to optimize the information content in the rotorcraft response measurements but also be properly conditioned such that the highest frequency content of the flight-test inputs is consistent with the frequency range of applicability of the model. Examples have also been given to illustrate the potentials of using multi-axis test inputs to enhance the parameter identifiability.

Also discussed in great length are the benefits of using frequency sweeps as input-test signals for identification of frequency-response for the rotorcraft and for subsequent fitting of parametric transfer-function models. The frequency sweep provides a good control over the frequency range of interest and it lends itself naturally to nonparametric frequency-domain identification. Analytical modeling and understanding of the physics involved in rotorcraft flight dynamics, especially understanding the limitation of lower-order models, can be more important than merely relying on the identification algorithms in the final stage of fitting parametric transfer-function models to the flight-extracted frequency response data.

#### Appendix: Pilot Comments on Frequency Sweep Inputs in BHTI 214ST Helicopter

Pilots: CW4 Robert A. Williams and Cpt. Randy Cason, USAEFA Edwards AFB, CA

Two Flights Completed 2 August 1985  
Hover Flight 1.2 hours  
Level Forward Flight 90 KCAS 1.6 hours

#### Recommendations

- A. Recommend that yaw inputs be performed prior to other inputs since the yaw rates were very low and it will aid in the pilot learning curve. The test should be done in order of increasing difficulty: yaw, collective, longitudinal, and then lateral inputs.
- B. Recommend that aircraft gross weight be at a minimum during the collective inputs. Maximum gross weight for the Bell 214ST is 17,500 lb and the test was conducted at approximately 13,000 lb. Torque readings were consistently greater than 90% (above 100% constitutes an overtorque).
- C. Recommend that the pilot be "coached" during the input. It is very easy to remain at one frequency too long, having the engineer tell the pilot to dwell on a specific frequency longer or increase frequency during a data run aided data acquisition. This assumes the engineer has real time data.
- D. Recommend that the copilot or flight test engineer coach the pilot for the low frequency responses by counting seconds for timing the quarter period. This should only be done for the lowest frequencies. It was found that if the copilot tried counting at the higher frequency, it only mixed up the pilot and resulted in the pilot following the copilot's counting rather than increasing the frequency as required by the test.
- E. Recommend that pilots practice the inputs utilizing external power supply (hydraulic and electrical power) on the ground prior to testing. This should significantly reduce test flight time.
- F. Recommend a "scope" with "freeze" capability be installed in the test aircraft unless "real time" TM is available.
- G. Recommend that the test team be briefed on all "aircraft" natural frequencies below 4.0 Hz and any resultant problems which may be encountered at these frequencies.

- H. During flights that require longitudinal inputs the instrumented A/S boom must be monitored closely for deflection beyond limits or removed.

#### References

1. Davis, J. M., Bennett, R. L., and Blankenship, B. L., "Rotorcraft Flight Simulation with Aeroelastic Rotor and Improved Aerodynamic Representation," USAAMRDL-TR-74-10B, June 1974.
2. Anderson, W. D., Conner, F., Kretsinger, P., and Reaser, J. S., "Rexor Rotorcraft Simulation Model," U.S. Army Air Mobility R&D Lab TR-76-28A, June 1976.
3. Johnson, W., "A Comprehensive Analytical Model of Rotorcraft Aerodynamics and Dynamics," Part I: Analysis Development, NASA TM 81182, June 1980.
4. "Parameter Estimation Techniques for Applications in Aircraft Flight Testing," NASA TN D-7647, April 1974 (Proceedings of Symposium held at NASA FRC, Edwards, CA, April 1973).
5. "Methods for Aircraft State and Parameter Identification," AGARD-CP-172, Nov. 1974.
6. "Parameter Identification," AGARD-LS-104, Nov. 1979.
7. Blake, B. B., and Alansky, I. B., "Stability and Control of the YUH-61A," Paper No. 75-31-27, 31st Annual National Forum of the American Helicopter Society, May 1975.
8. Kuczynski, W. A., Cooper, D. E., Twomey, W. J., and Howlett, J. J., "The Influence of Engine/Fuel Control Design on Helicopter Dynamics and Handling Qualities," Preprint No. 79-37, 35th Annual National Forum of the American Helicopter Society, May 1979.
9. Molusis, J. A., "Analytical Study to Define a Helicopter Stability Derivative Extraction Method," NASA CR-132371, Nov. 1974.
10. Hall, W. E. Jr., and Bryson, A. E. Jr., "Inclusion of Rotor Dynamics in Controller Design," J. Aircraft, Vol. 10, April 1973, pp. 200-206.
11. Chen, R. T. N., and Hindson, W. S., "Influence of High-Order Dynamics on Helicopter Flight-Control System Bandwidth," AIAA J. Guidance, Vol. 9, No. 2, March-April 1986, pp. 190-197.
12. Hilbert, K. B., Lebacqz, J. V., Hindson, W. S., "Flight Investigation of a Multi-variable Model-Following Control System for Rotorcraft," AIAA Paper 86-9779, presented at AIAA 3rd Flight Test Conf., April 2-4, 1986.
13. Ormiston, R. A., "Application of Simplified Inflow Models to Rotorcraft Dynamic Analysis," J. AHS, July 1976, pp. 34-37.
14. Johnson, W., "Influence of Unsteady Aerodynamics on Hingeless Rotor Ground Resonance," J. Aircraft, Vol. 19, No. 8, August 1982, pp. 668-673.
15. Pitt, D. M., and Peters, D. A., "Theoretical Prediction of Dynamic-Inflow Derivatives," VERTICA, Vol. 5, No. 1, 1981, pp. 21-34.
16. Carpenter, F. J., and Fridovich, B., "Effect of a Rapid-Pitch Increase on the Thrust and Induced-Velocity Response of a Full-Scale Helicopter Rotor," NACA TN-3044, November 1953.
17. Banerjee, D., and Hohenemser, K. H., "Optimum Data Utilization for Parameter Identification with Application to Lifting Rotors," J. Aircraft, Vol. 13, Dec. 1976, pp. 1014-1016.
18. Chen, R. T. N., and Hindson, W. S., "Influence of Dynamic Inflow on the Helicopter Vertical Response," submitted for publication in VERTICA, 1986.
19. Chen, R. T. N., Eulrich, B. J., and Lebacqz, J. V., "Development of Advanced Techniques for the Identification of V/STOL Aircraft Stability and Control Parameters," Cornell Aeronautical Laboratory, Inc., Buffalo, N.Y., CAL Report No. BM-2820-F-1, Aug. 1971.
20. Kaletka, J., "Rotorcraft Identification Experience," in AGARD-LS-104, Nov. 1979, pp. 7-1 to 7-32.
21. Kaletka, J., "Practical Aspects of Helicopter Parameter Identification," submitted for publication, 1985.

22. Molusis, J. A., "Helicopter Stability Derivative Extraction from Flight Data Using a Bayesian Approach to Estimation," J. Amer. Helicop. Soc., July 1973.
23. Molusis, J. A., "Rotorcraft Derivative Identification from Analytical Models and Flight Test Data," AGARD-CP-172, Nov. 1974.
24. Gould, D. G., and Hindson, W. S., "Estimates of the Stability Derivatives of a Helicopter and a V/STOL Aircraft from Flight Data," AGARD-CP-172, Nov. 1974.
25. Tomaine, R. L., "Flight Data Identification of Six Degree-of-Freedom Stability and Control Derivatives of a Large Crane," NASA TMX-73958, Sept. 1976.
26. Hall, W. E., Gupta, N. K., and Hansen, R. S., "Rotorcraft System Identification Techniques for Handling Qualities and Stability and Control Evaluation," Preprint No. 78-30, 34th Annual Forum of the American Helicopter Society, May 1978.
27. Padfield, G. D., Thorne, R., Murray-Smith, D., Black, C., and Caldwell, A. E., "UK Research into System Identification for Helicopter Flight Mechanics," Paper No. 82, 11th European Rotorcraft Forum, London, England, 10-13 September 1985.
28. Fu, K.-H., and Marchand, M., "Helicopter System Identification in the Frequency Domain," 9th European Rotorcraft Forum, Stresa, Italy, Sept. 1983.
29. Tischler, M. B., Leung, J. G. M., and Dugan, D. C., "Identification and Verification of Frequency-Domain Models for XV-15 Tilt-Rotor Aircraft Dynamics," European Rotorcraft Forum, September 1985, The Hague, Holland.
30. Tischler, M. B., Leung, J. G. M., and Dugan, D. C., "Frequency-Domain Identification of XV-15 Tilt-Rotor Aircraft Dynamics in Hovering Flight," AIAA Paper 83-2695, AIAA/AHS 2nd Flight Testing Conference, Las Vegas, November 1983. (Also published in condensed version in J. Amer. Helicopter Soc., Vol. 30, No. 2, April 1985, pp. 38-48.)
31. "CTRL-C, A Language for the Computer-Aided Design of Multivariable Control Systems," User's Guide (2.3), System Control Technology, Palo Alto, CA, 9 March 1984.
32. "MATRIXX," User's Guide (Version 5.0), Integrated Systems Inc., Palo Alto, CA, October 1985.
33. Mehra, R. K., and Gupta, N. K., "Status of Input Design for Aircraft Parameter Identification," AGARD-CP-172, Nov. 1974.
34. Chen, R. T. N., "Input Design for Aircraft Parameter Identification Using Time-Optimal Control Formulation," AGARD-CP-172, Nov. 1974.
35. Plaetschke, E., and Schulz, G., "Practical Input Signal Design," AGARD-LS-104, Nov. 1979.
36. Hindson, W. S., Hilbert, K. B., Tucker, G. E., Chen, R. T. N., and Fry, E. B., "New Capabilities and Recent Research Programs of the NASA/Army CH-47B Variable-Stability Helicopter," presented at the 42nd Annual National Forum of the American Helicopter Society, June 1986.
37. Hoh, R. H., Myers, T. T., Ashkenas, I. L., Ringland, R. F., and Craig, S., "Development of Handling Quality Criteria for Aircraft with Independent Control of Six Degrees of Freedom," Air Force Wright Aero Lab TR-81-3027, April 1981.
38. Jex, H. R., Hogue, H. R., Magdaleno, R. E., Gelhausen, P. A., "Dynamic Flight-Tests of the Skyship-500 Airship," System Technology, Inc. TR-1151-4, March 1986.
39. Tischler, M. B., Fletcher, J., Diekmann, V., Williams, R. A., and Cason, R., "Frequency-Sweep Flight Test of a Bell 214-ST Helicopter," work in preparation (1986).
40. Aponso, B. L., DiMarco, R. J., and Mitchell, D. G., "Obtaining Bandwidth from Frequency Sweep Data Using the STI Frequency Domain Analysis (FREDA) Package," System Technology, Inc. Working Paper 1194-100-1, Sept. 1985.
41. Hoh, R. H., Mitchell, D. G., Ashkenas, I. L., Aponso, B. L., Ferguson, S. W., Rosenthal, T. J., Key, D. L., and Blanken, C. L., "Proposed Airworthiness Design Standard: Handling Qualities Requirements for Military Rotorcraft," System Technology, Inc. TR-1194-2, 20 Dec. 1985.
42. Tayler, L. W., Jr., "Application of a New Criterion for Modeling Systems," AGARD-CP-172, Nov. 1974.

Table 1a F and G matrices for 10th order teetering rotor helicopter in hover

Matrix F									
0	0	1.0	0	0	0	0	0	0	0
0	0	0	1.0	0	0	0	0	0	0
-4.534	-571.6	-21.18	-53.95	0	0	-22.02	-56.69	0.1116	-0.3493
560.7	-22.67	53.78	-20.77	0	0	56.45	-21.55	-0.342	-0.1036
0	0	0	0	0	0	1.0	0	0	0
0	0	0	0	0	0	0	1.0	0	0
4.33	-2.627	-0.09731	-0.04358	0	0	-0.1122	-0.05643	0.001908	-0.001641
13.14	21.65	0.2083	-0.4865	0	0	0.2822	-0.5612	-0.008207	-0.00954
-22.27	13.52	0.5009	0.2243	-32.2	0	2.344	1.282	-0.00982	0.00845
13.52	22.27	0.2243	-0.5009	0	32.2	1.811	-2.344	-0.008452	-0.00982

Matrix G

0
0
571.7
-10.1
0
0
2.627
9.648
-13.52
9.931

Eigenvalues

Real	Imag.
-10.62	±51.76
-9.288	±3.519
-1.226	
-1.832	
-0.01475	±0.5454
0.1330	±0.3736

State vector =  $(a_1 \ b_1 \ \dot{a}_1 \ \dot{b}_1 \ \theta \ \phi \ q \ p \ u \ v)'$

Control =  $A_{10}$

Table 1b F and G matrices for simplified, quasi-static 6th order helicopter model

Matrix F					
0	0	1.0	0	0	0
0	0	0	1.0	0	0
0	0	-0.4557	0.3538	0.004082	0.0006605
0	0	-1.877	-2.262	0.004030	-0.02070
-32.2	0	4.110	-0.8290	-0.02100	-0.003391
0	32.2	-0.4106	-4.094	0.004138	-0.02129

Matrix G

0
0
0.2538
32.06
-1.305
32.98

Eigenvalues

Real	Imag.
-0.9909	
-2.009	
-0.01147	±0.5408
0.1315	±0.3713

State vector =  $(\theta \ \phi \ q \ p \ u \ v)'$

control =  $A_{10}$

Table 2 Three vertical dynamic models

a. Dynamic inflow-flap-vertical motion

$$\begin{Bmatrix} \dot{v} \\ \dot{\beta} \\ \dot{w} \end{Bmatrix} = \begin{bmatrix} -8.225 & 0 & -109.466 & 5.473 \\ 0 & 0 & 1 & 0 \\ -1.155 & -607.421 & -26.116 & 1.155 \\ -0.069 & -514.579 & -3.924 & 0.069 \end{bmatrix} \begin{Bmatrix} v \\ \beta \\ \dot{\beta} \\ w \end{Bmatrix} + \begin{bmatrix} 1311.485 \\ 0 \\ 629,004 \\ 94.510 \end{bmatrix} \theta_0$$

per rad

$$\lambda_1 = \begin{cases} -10.567 \pm j 17.475 \\ -12.855 \\ -0.284 \end{cases}$$

b. Constant inflow-flap-vertical motion

$$\begin{Bmatrix} \dot{\beta} \\ \dot{w} \end{Bmatrix} = \begin{bmatrix} 0 & 1 & 0 \\ -607.421 & -26.116 & 0.387 \\ -514.579 & -3.924 & 0.023 \end{bmatrix} \begin{Bmatrix} \beta \\ \dot{\beta} \\ w \end{Bmatrix} + \begin{bmatrix} 0 \\ 444.874 \\ 83.51 \end{bmatrix} \theta_0$$

$$\lambda_1 = \begin{cases} -12.893 \pm j 20.837 \\ -0.308 \end{cases}$$

c. Quasi-static vertical dynamics

$$\dot{w} = -0.304w - 293.338 \theta_0 \quad \lambda_1 = -0.304$$

Table 3 Vertical acceleration to collective transfer-functions of the three vertical dynamic models

$$a. \quad -\frac{a_z}{\delta_c} = \frac{-3 s^4 - 22 s^3 + 8771 s^2 + 47630 s}{s^4 + 34.3 s^3 + 698.3 s^2 + 5556 s + 1520.3}$$

4th-order model  
(dynamic inflow-flap-vertical motion)

$$= \frac{-3(0)(-52.611)(54.468)(5.411)}{[0.518; 20.421]^*(12.855)(0.284)}$$

$$b. \quad -\frac{a_z}{\delta_c} = \frac{-2.7 s^3 - 14.1 s^2 + 5791.4 s}{s^3 + 26.093 s^2 + 608.334 s + 184.853}$$

3rd-order model  
(no inflow dynamics)

$$= \frac{-2.7(0)(-43.661)(48.873)}{[0.526; 24.503](0.308)}$$

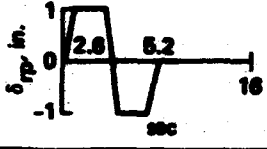
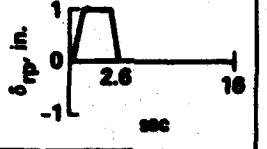
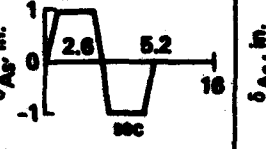
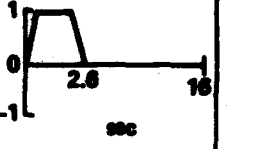
$$c. \quad -\frac{a_z}{\delta_c} = \frac{12.784 s}{s + 0.304}$$

1st-order model  
(quasi-static model)

$$= \frac{12.784(0)}{(0.304)}$$

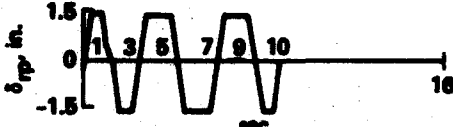
\*[c; u<sub>n</sub>]

Table 4 Comparison of aileron inputs and rudder inputs

CASE		RUDDER INPUTS		AILERON INPUTS	
		DOUBLET	PULSE	DOUBLET	PULSE
PARAMETER					
	PARA.	(UNIT IN rad, sec)	$\sigma_{min}$ (16 sec DATA)		
$L_p$	-2.32	0.4455	0.3123	0.0402	0.0558
$L_r$	1.122	0.3733	0.2825	0.1715	0.1196
$L_\beta$	-6.918	1.1655	0.8253	0.1278	0.1562
$L_{\delta_r}$	0.2761	0.0201	0.0169	-	-
$L_{\delta_s}$	3.631	-	-	0.0362	0.0529
$N_p$	-0.03211	0.0785	0.0554	0.0064	0.0085
$N_r$	-0.1232	0.0856	0.0462	0.0306	0.0211
$N_\beta$	1.238	0.2054	0.1462	0.0196	0.0151
$N_{\delta_r}$	-0.2121	0.0033	0.00278	-	-
$N_{\delta_s}$	0.01685	-	-	0.0051	0.0069
$(Y_p/V_0) + \alpha_0$	0.03331	0.0437	0.0224	0.0107	0.0133
$(Y_r/V_0) - 1$	-0.9882	0.0353	0.0140	0.0149	0.0086
$Y_\beta/V_0$	-0.06146	0.1155	0.0644	0.0341	0.0475
$Y_{\delta_r}/V_0$	-0.00522	0.00299	0.00440	-	-
$Y_{\delta_s}/V_0$	-0.00285	-	-	0.0162	0.0208
$\Sigma \sigma_j^2$		1.7656	0.5793	0.0518	0.0484

VARIABLES:  $p$  0.1 deg/sec,  $r$  0.02 deg/sec,  $\phi$  0.075 deg,  $\beta$  0.075 deg  
 MEASUREMENT ERROR,  $\sigma$ :

Table 5 Suboptimal inputs - simultaneous use of aileron and rudder

CASE PARAMETER		SUBOPTIMAL INPUT I		SUBOPTIMAL INPUT II	
					
PARA.	VALUE (UNIT IN rad, sec)	$\sigma_{min}$ (16 sec DATA)			
$L_p$	-2.32	0.02183		0.0240	
$L_r$	1.122	0.04170		0.0474	
$L_\beta$	-6.916	0.07004		0.08885	
$L_{\delta_r}$	0.2761	0.00835		0.00821	
$L_{\delta_s}$	3.631	0.02884		0.0282	
$N_p$	-0.03211	0.00373		0.00420	
$N_r$	-0.1232	0.00741		0.00844	
$N_\beta$	1.238	0.01185		0.01194	
$N_{\delta_r}$	-0.2121	0.000788		0.000732	
$N_{\delta_s}$	0.01685	0.00462		0.00483	
$(Y_p/V_0) + \alpha_0$	0.0331	0.00410		0.00477	
$(Y_r/V_0) - 1$	-0.9882	0.00577		0.00608	
$Y_\beta/V_0$	-0.08146	0.01225		0.01380	
$Y_{\delta_r}/V_0$	0.00522	0.00185		0.00147	
$Y_{\delta_s}/V_0$	-0.00285	0.00632		0.00742	
$\Sigma \sigma_i^2$		0.00841		0.00899	

VARIABLES:  $p$   $r$   $\phi$   $\beta$   
 MEASUREMENT ERROR,  $\sigma$ : 0.1 deg/sec 0.02 deg/sec 0.075 deg 0.075 deg

Table 6 Recommended practical aileron and rudder input

PARAMETER		CASE		
			PARA.	(UNIT IN rad, sec)
$L_p$	-2.32			0.033
$L_r$	1.122			0.076
$L_\beta$	-6.916			0.006
$L_{\delta_r}$	0.2761			0.008
$L_{\delta_s}$	3.631			0.006
$N_p$	-0.03211			0.0008
$N_r$	-0.1232			0.013
$N_\beta$	1.238			0.014
$N_{\delta_r}$	-0.2121			0.0014
$N_{\delta_s}$	0.01685			0.0009
$(Y_p/V_0) + a_0$	0.03331			0.0079
$(Y_r/V_0) - 1$	-0.9882			0.0006
$Y_\beta/V_0$	-0.06146			0.024
$Y_{\delta_r}/V_0$	0.00522			0.0034
$Y_{\delta_s}/V_0$	-0.00285			0.012
$\Sigma \sigma_1^2$				0.017

VARIABLES: p r  $\phi$   $\beta$   
 MEASUREMENT ERROR,  $\sigma$ : 0.1 deg/sec 0.02 deg/sec 0.075 deg 0.075 deg

Table 7 Several parametric models identified from the CH-47B flight-generated  $-(a_2/s_0)$  transfer-function

System order	Frequency range (r/s)	Transfer function	Fitting error index
a. 1	0.1 to 3.0	$\frac{8.542 s}{s + 0.160}$	18.054
b. 1	0.1 to 20.0	$\frac{11.948 s}{s + 0.228}$	666.604
c. 3	0.1 to 20.0	$\frac{-0.233 s^3 + 10.827 s^2 + 1943.266 s}{s^3 + 6.922 s^2 + 197.617 s + 28.066} e^{-0.024s}$	116.015
d. 4	0.1 to 20.0	$\frac{-0.233(0)(-117.54)(71.023)}{(0.143)(0.242; 14.023)} e^{-0.024s}$	64.191
e. 4	0.1 to 20.0	$\frac{-12.004 s^3 + 13185.306 s^2 + 182672.75 s}{s^4 + 82.680 s^3 + 849.034 s^2 + 19391.045 s + 3029.032} e^{-0.031s}$	30.381
f. 5	0.1 to 20.0	$\frac{-12.004(0)(-1112.1)(13.684)}{(0.157)(74.787)(0.241; 16.048)} e^{-0.031s}$	21.698
		$\frac{-0.607 s^4 + 24.247 s^3 + 5361.57 s^2 + 27066.53 s}{s^4 + 26.456 s^3 + 372.992 s^2 + 2961.33 s + 398.250} e^{-0.011s}$	
		$\frac{-0.607(0)(-118.06)(5.186)(72.895)}{(0.137)(14.665)(0.414; 14.088)} e^{-0.011s}$	
		$\frac{-0.0436 s^5 - 12.666 s^4 + 663.797 s^3 + 69538.406 s^2 + 180763.83 s}{s^5 + 18.596 s^4 + 534.796 s^3 + 4998.873 s^2 + 24461.41 s + 2718.457} e^{-0.017s}$	
		$\frac{-0.0436(0)(-88.848)(2.671)(54.172)(322.68)}{(0.114)(0.176; 19.786)(0.738; 7.813)} e^{-0.017s}$	

\*[ $\tau; \eta_1$ ]

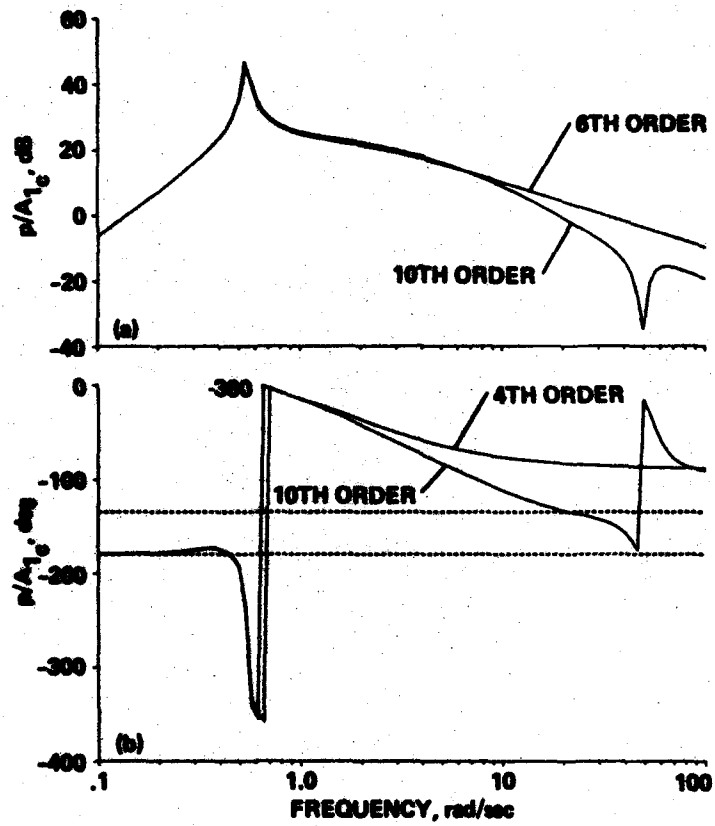


Fig. 1 Comparison of the frequency responses of  $P/A_1$  for 10th and 6th order systems.

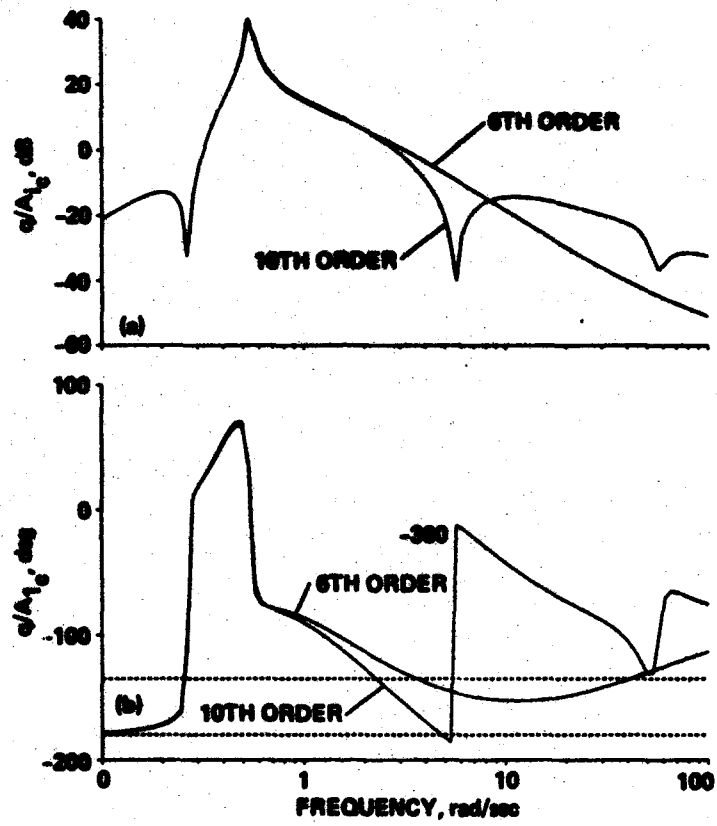


Fig. 2 Comparison of the frequency responses of  $q/A_1$  for 10th and 6th order systems.

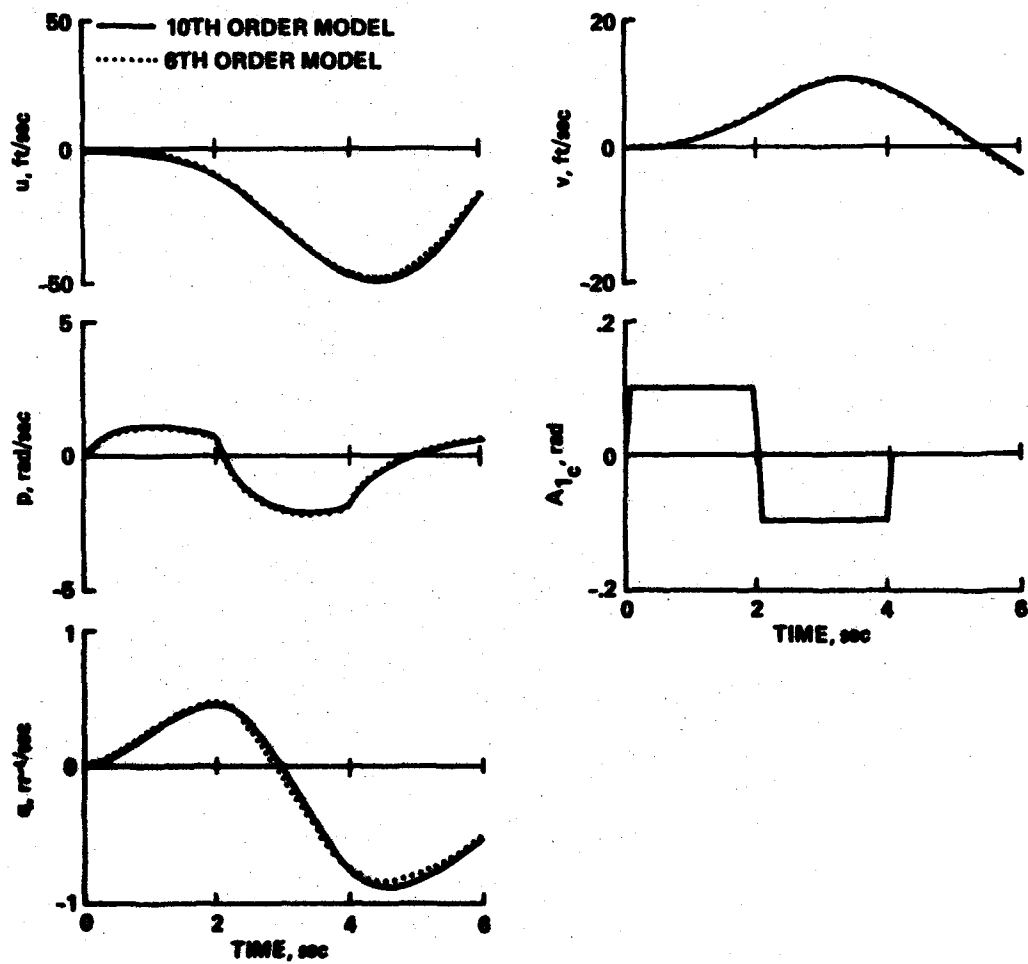


Fig. 3 Comparison of the transient responses of the 10th and 6th order models to a low frequency (1.6 rad/sec) doublet input.

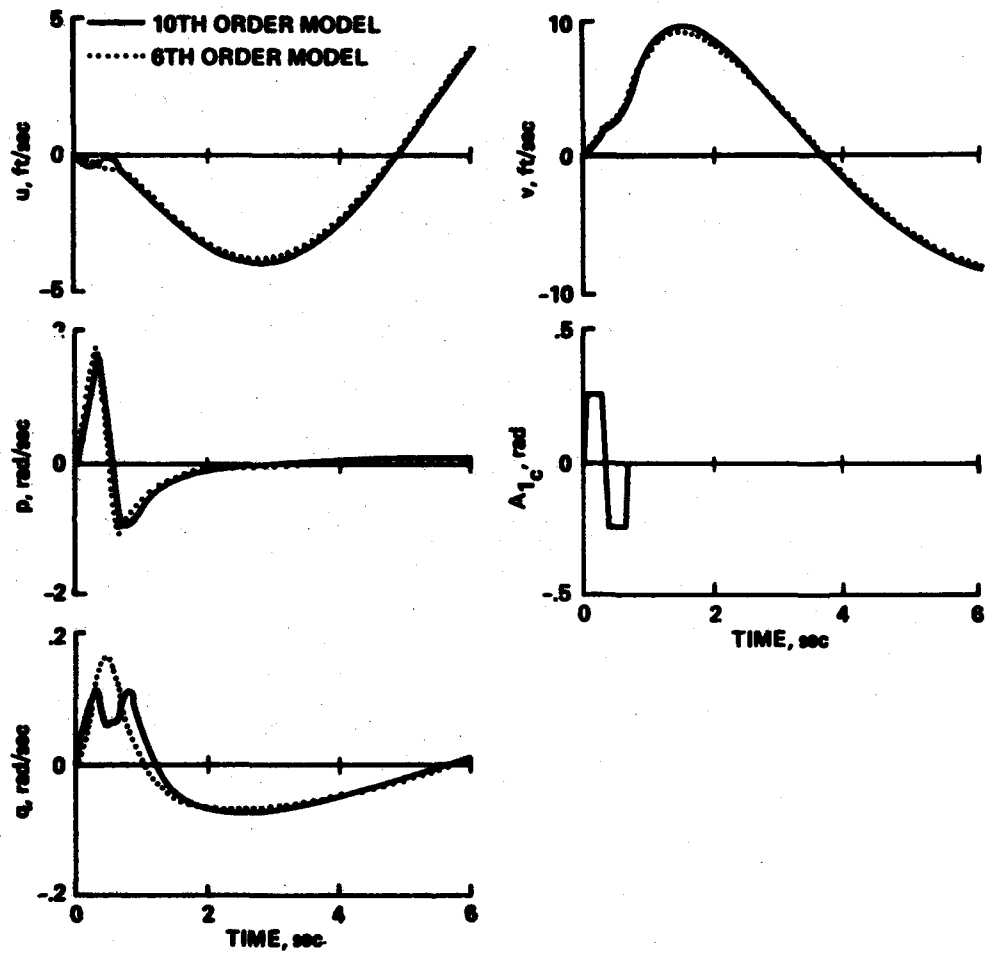


Fig. 4 Comparison of the transient responses of the 10th and 6th order models to a high frequency (9 rad/sec) doublet input.

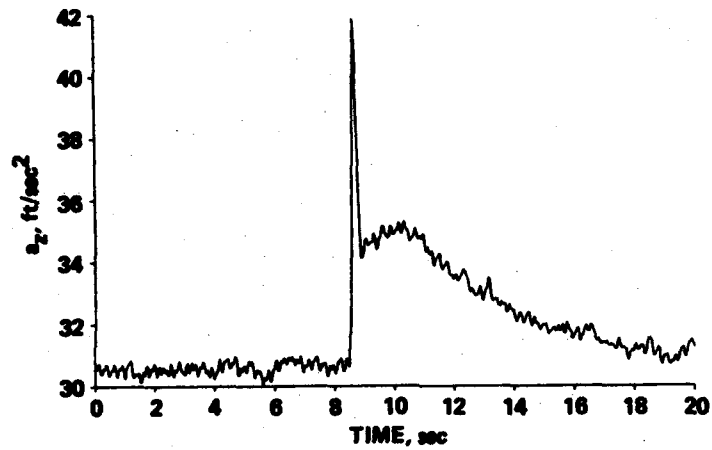


Fig. 5 Vertical acceleration response of the CH-47B helicopter to a step collective input,  $\Delta\delta_c = 0.62$  in. ( $\Delta\theta_0 = 0.0201$  rad).

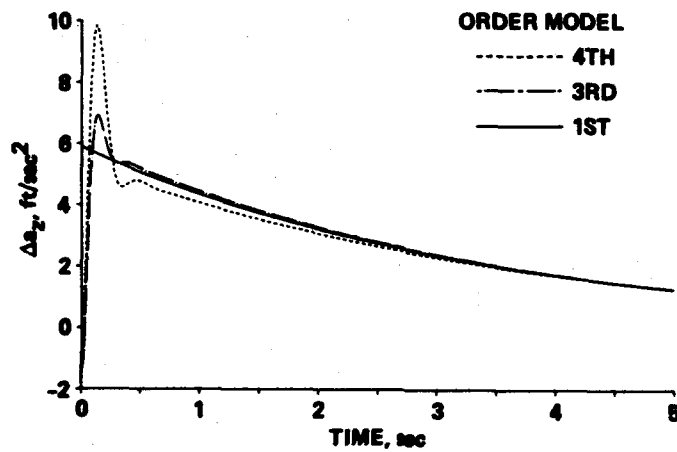


Fig. 6 Calculated vertical acceleration response to 0.62 in. (0.0201 rad) step collective input: (a) 4th-order model, (b) 3rd-order model, (c) 1st-order, quasi-static model.

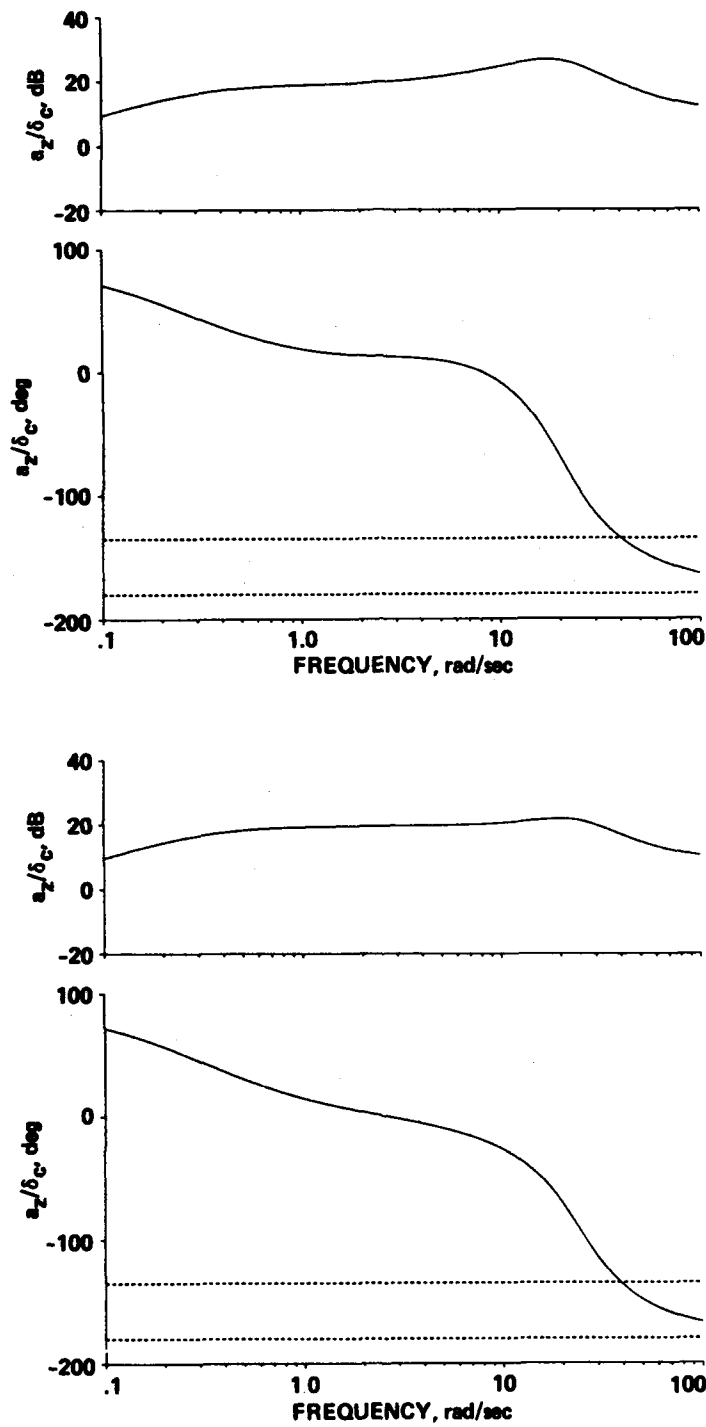


Fig. 7 Calculated frequency response of vertical acceleration ( $\text{ft/s}^2$ ) to collective input (in.): (a) 4th-order model, (b) 3rd-order model, (c) 1st-order, quasi-static model.

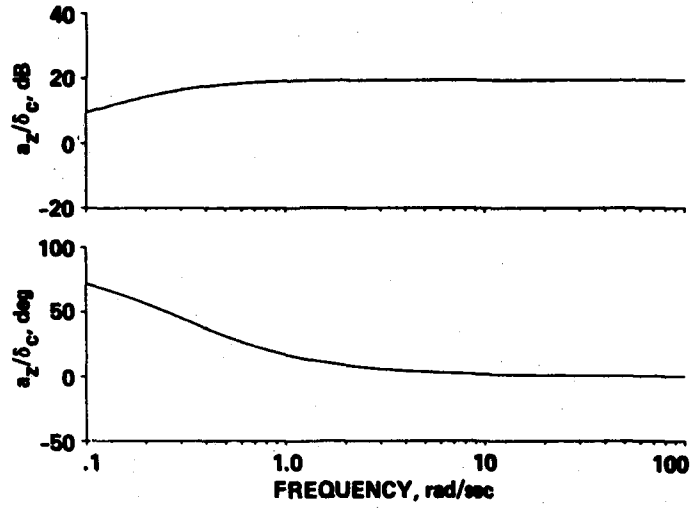


Fig. 7 Concluded.

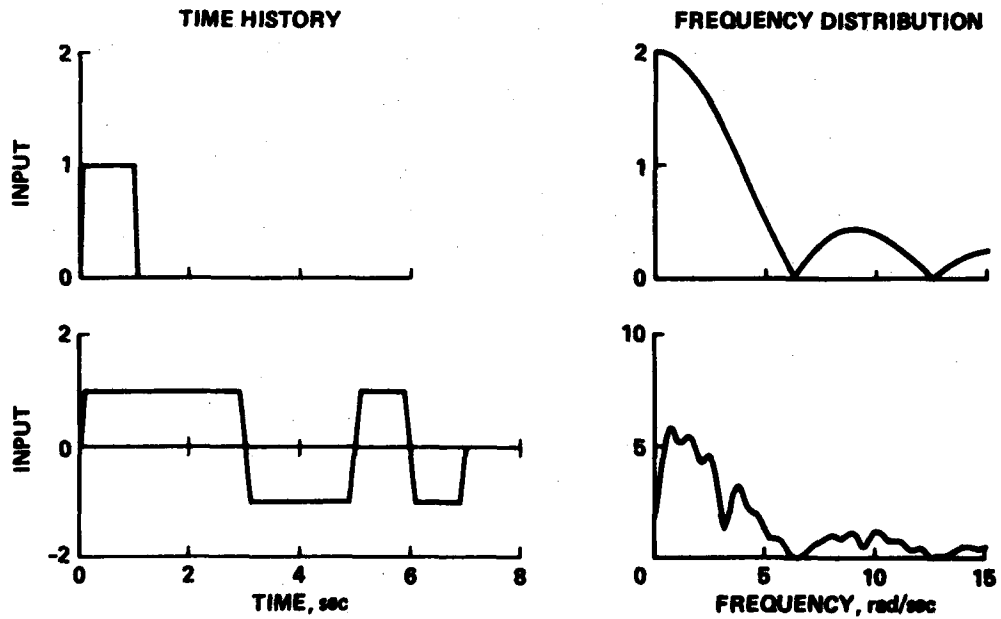


Fig. 8(a) Time history and frequency distribution of a pulse and a "3-2-1-1" multistep test input.

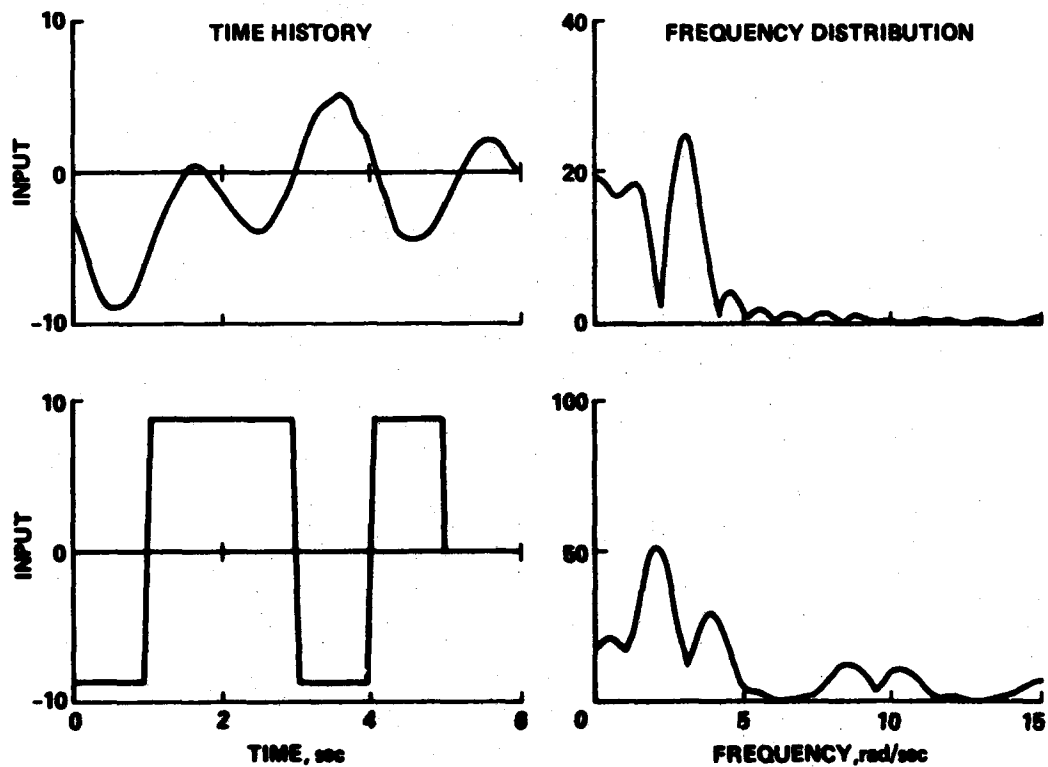


Fig. 8(b) Time history and frequency distribution of a smooth test input and a multistep test input.

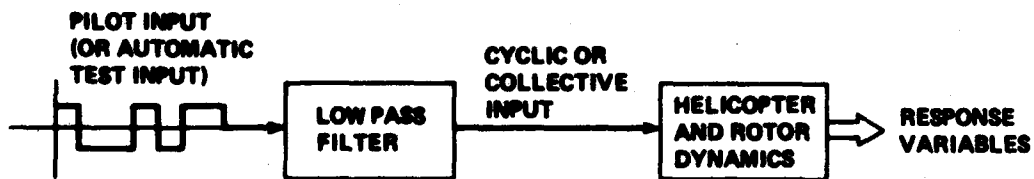


Fig. 9 Schematic diagram for input signal conditioning.

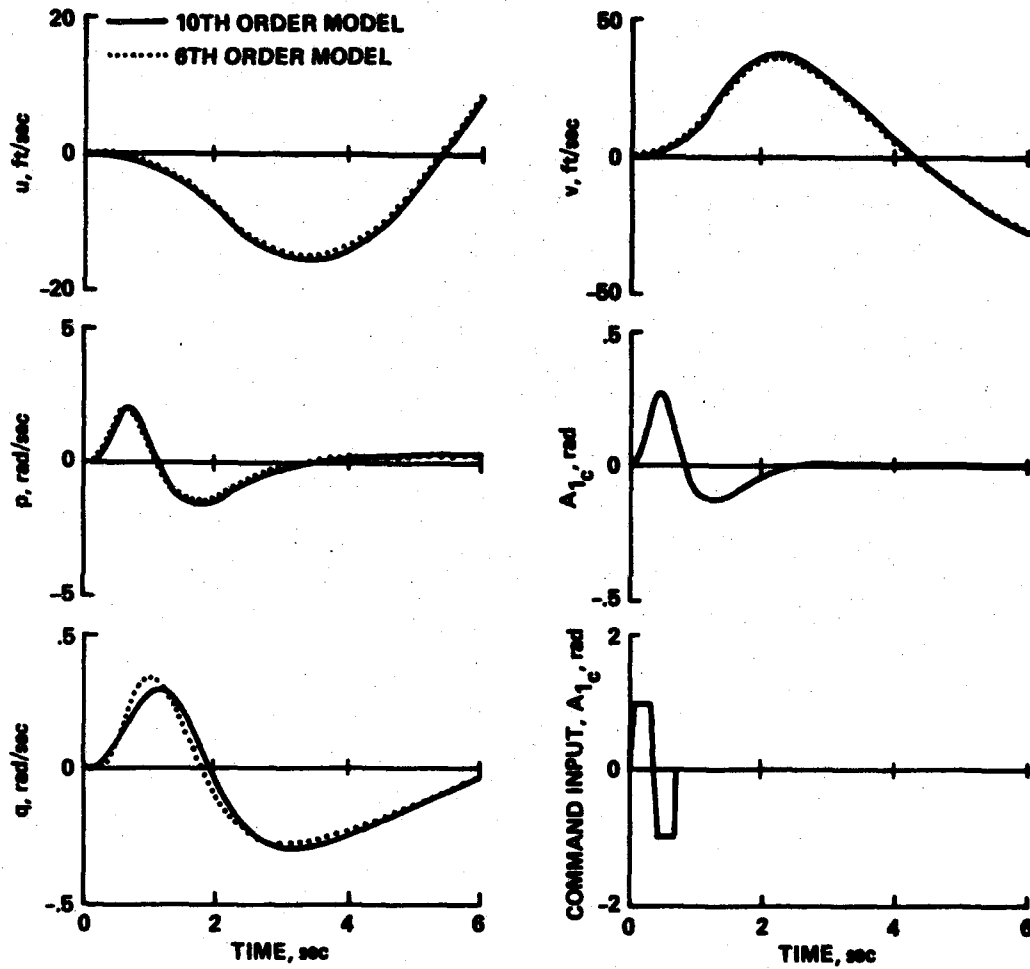


Fig. 10 Comparison of the transient responses of the 10th and 6th order models to a high frequency (9 rad/sec) doublet shaped with a 2nd order filter ( $\omega_c = 2.5$  rad/sec,  $\zeta = 0.7$ ).

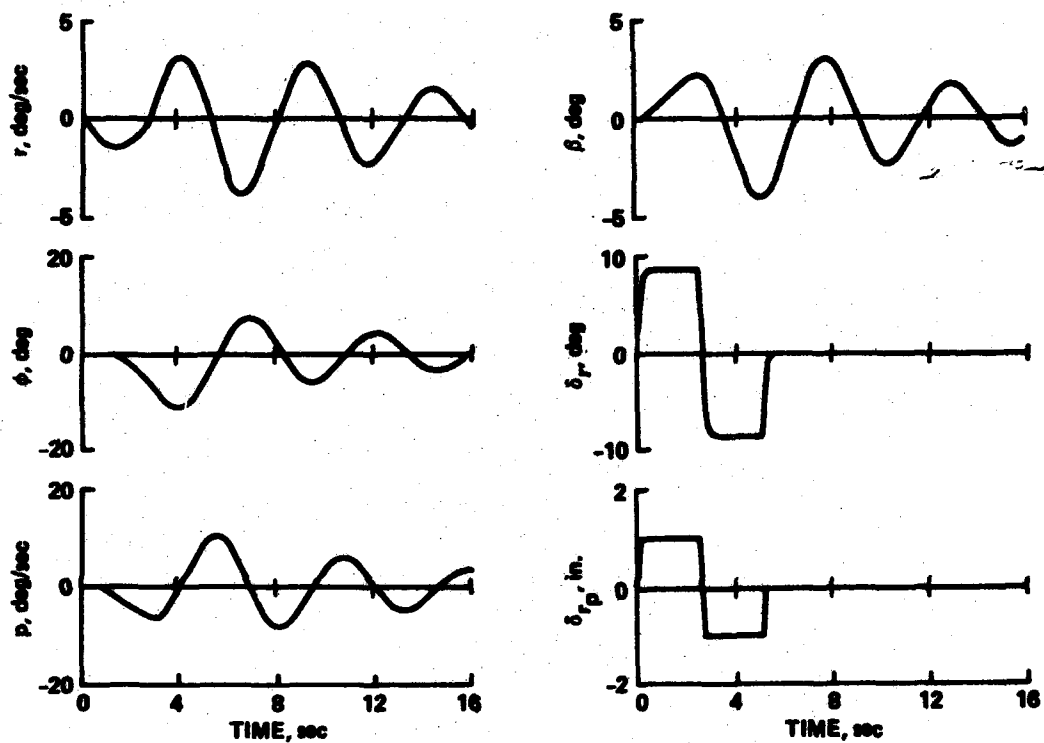


Fig. 11 Aircraft response to a rudder doublet input.

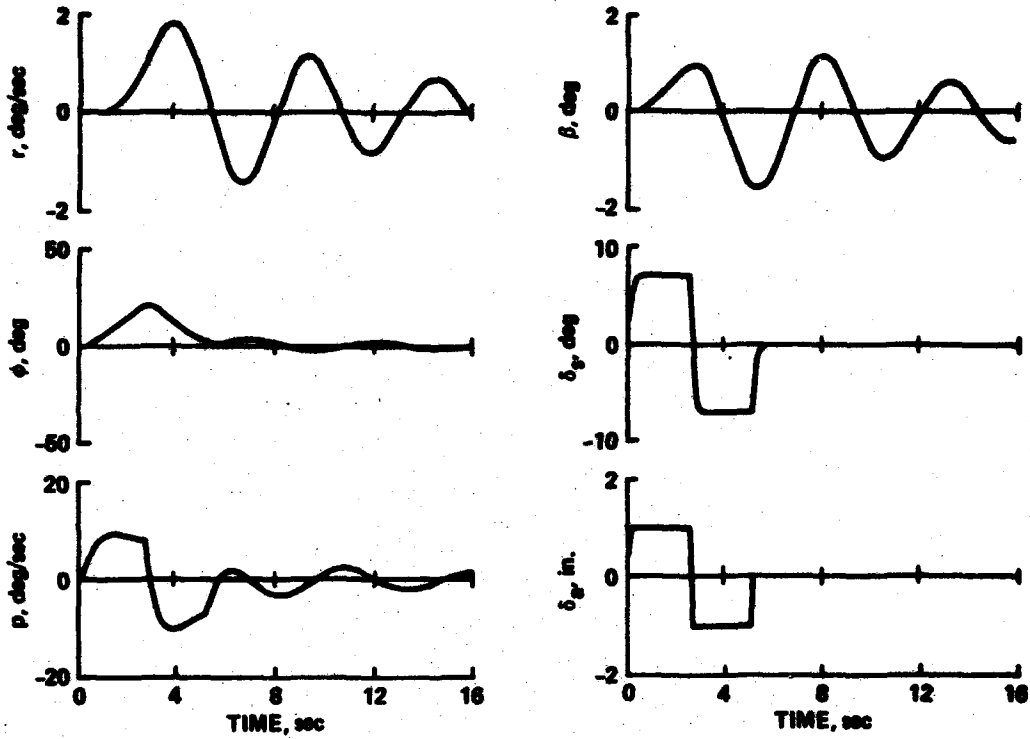


Fig. 12 Aircraft response to an aileron doublet input.

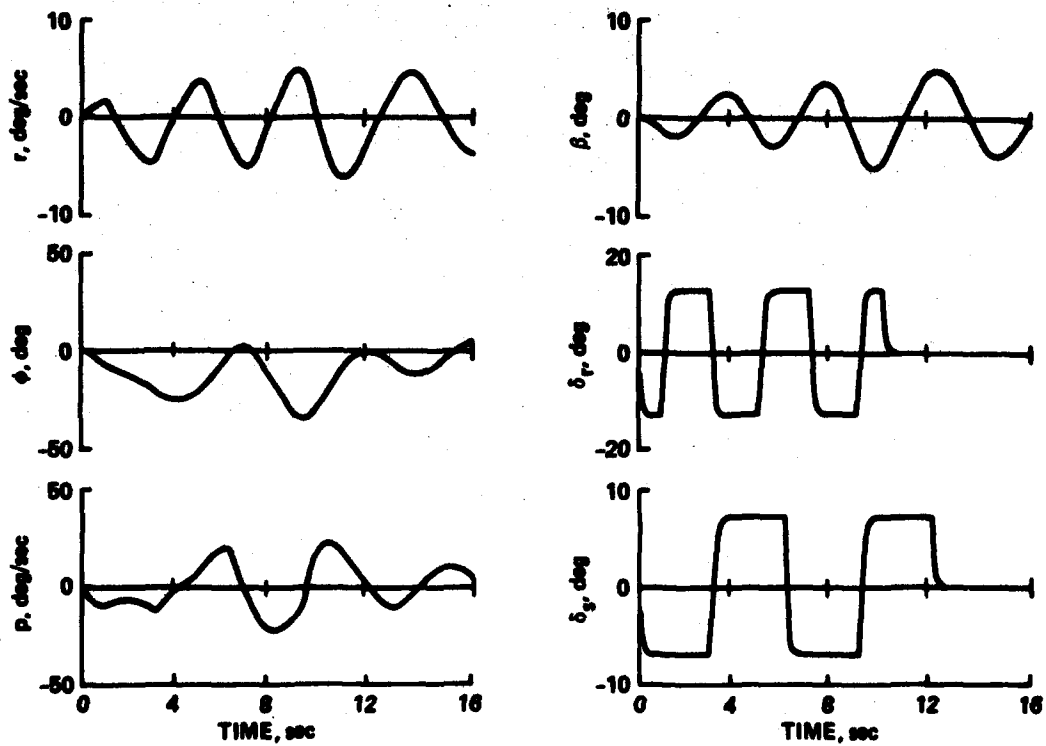


Fig. 13 Aircraft response to the lateral-directional suboptimal input II.

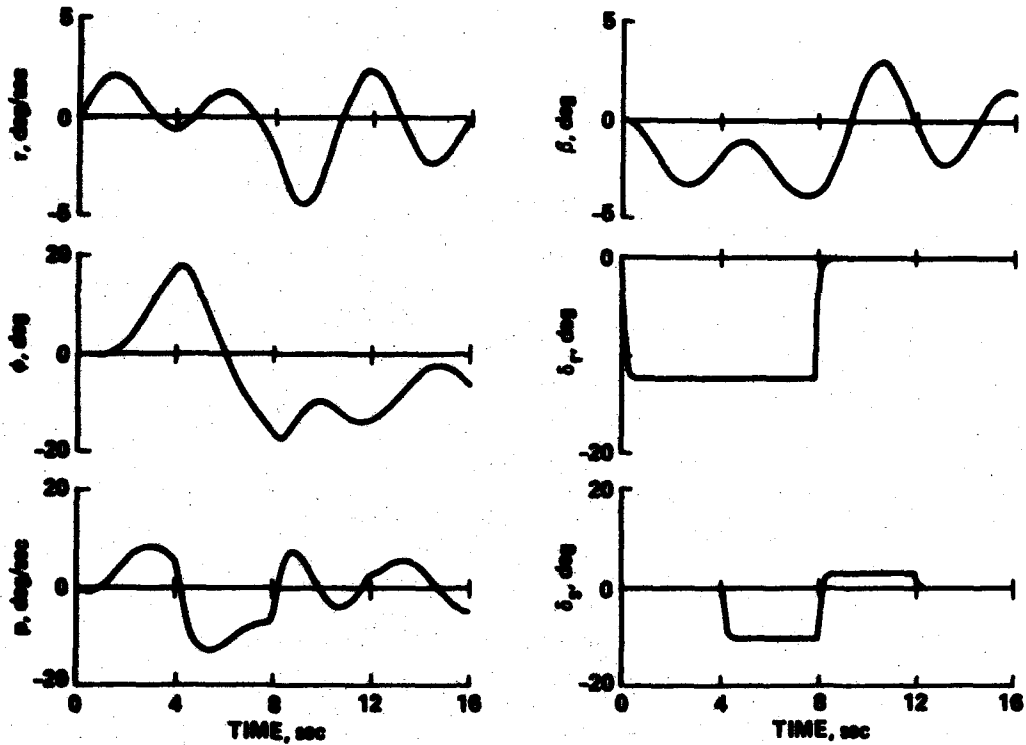


Fig. 14 Aircraft response to the recommended aileron and rudder input.

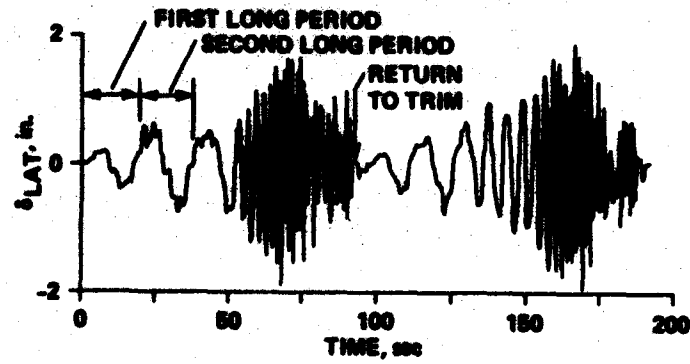


Fig. 15 Two lateral stick frequency sweeps in hover.

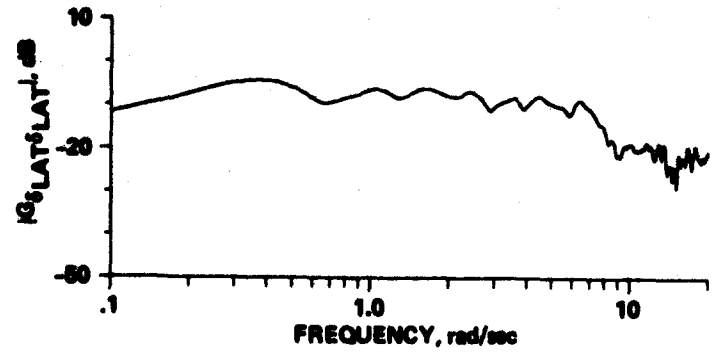


Fig. 16 Lateral stick input autospectrum.

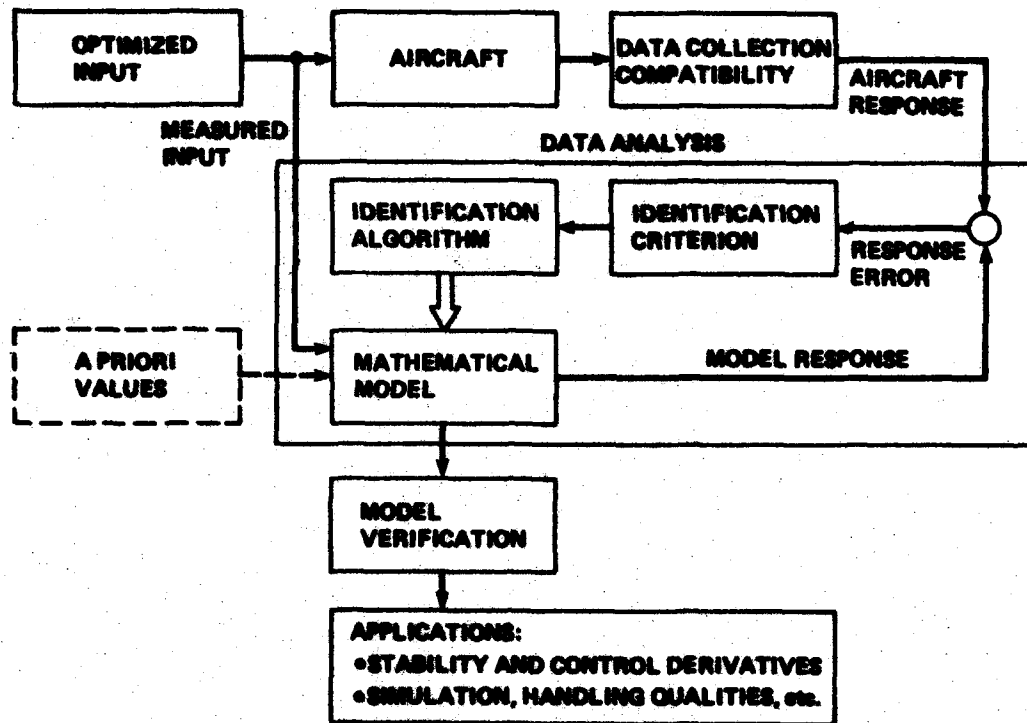


Fig. 17 System identification procedure (from Ref. 21).

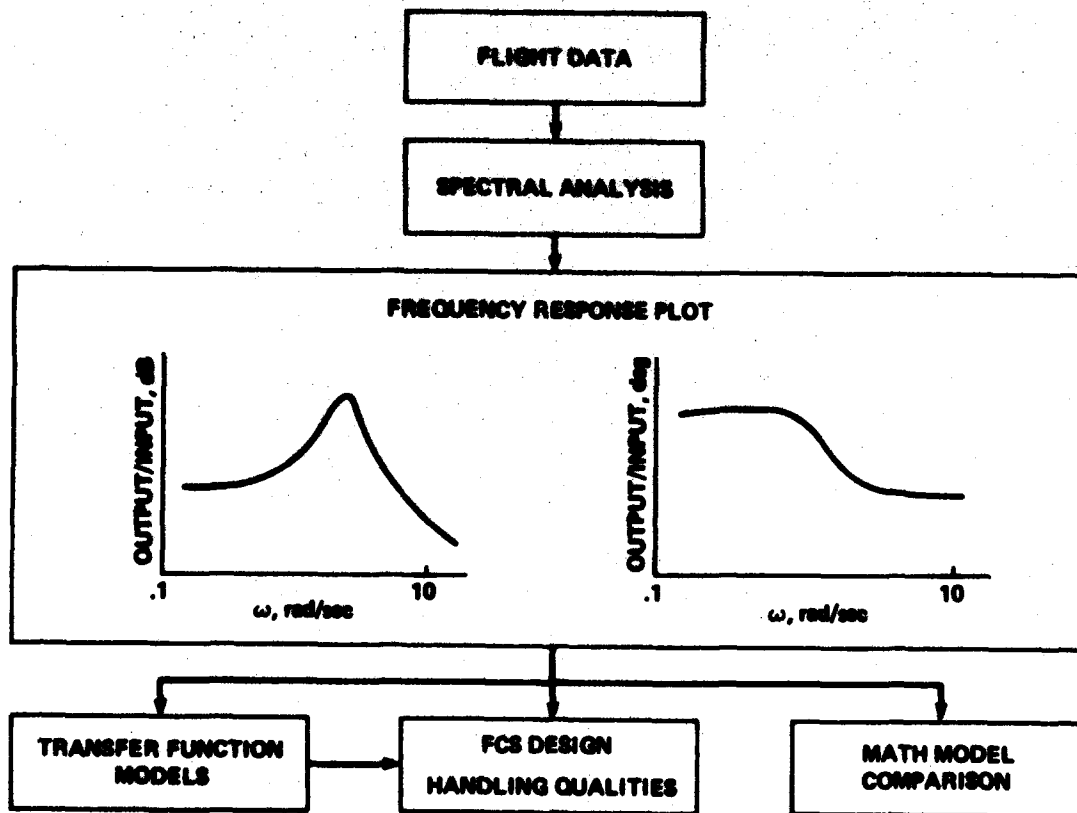


Fig. 18 Frequency-domain identification methodology.



Fig. 19 The XV-15 tilt-rotor aircraft in hover configuration.

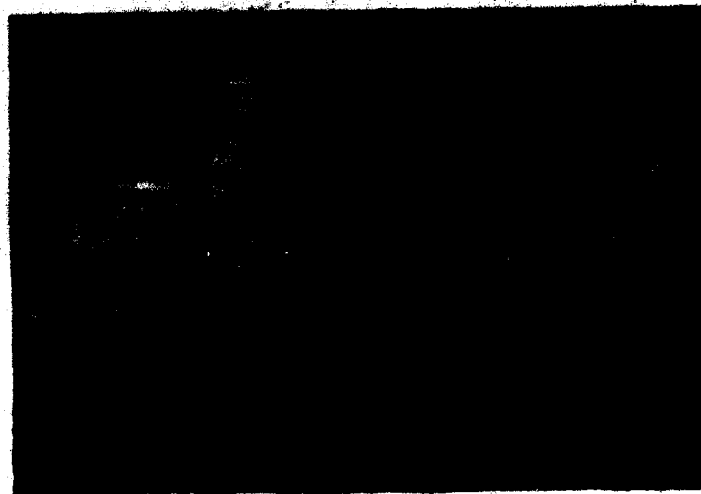


Fig. 20 Bell 214-ST helicopter.

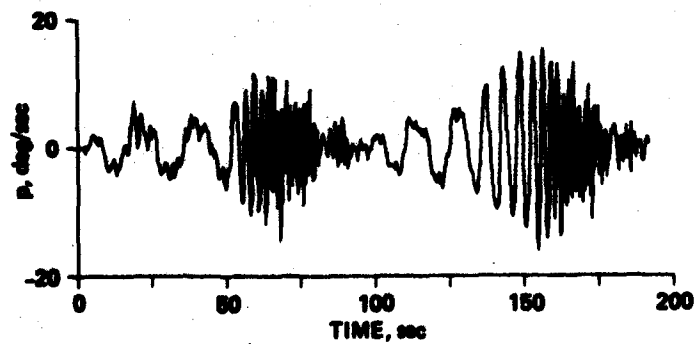


Fig. 21 Roll rate during the lateral stick frequency sweeps (Bell 214-ST).

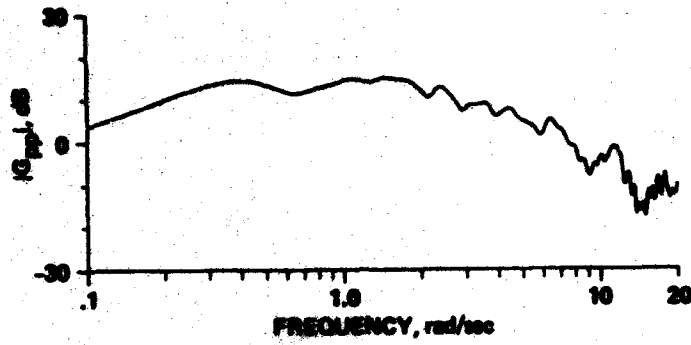


Fig. 22 Roll rate output autospectrum (Bell 214-ST).

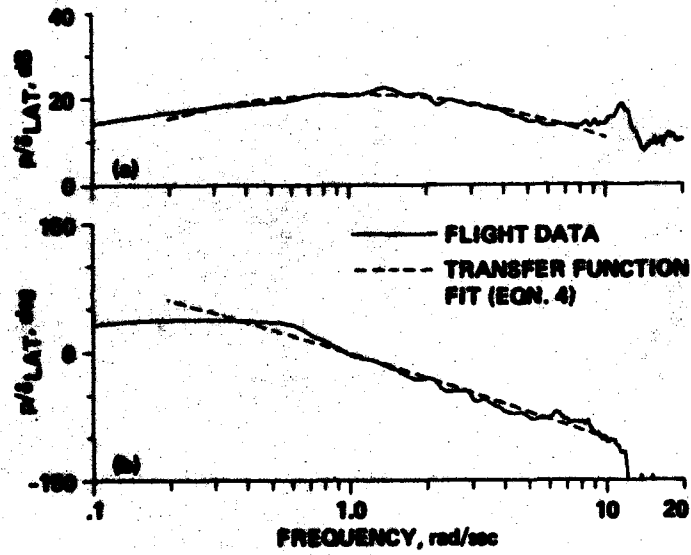


Fig. 23 Roll attitude response to lateral stick in hover (Bell 214-ST).

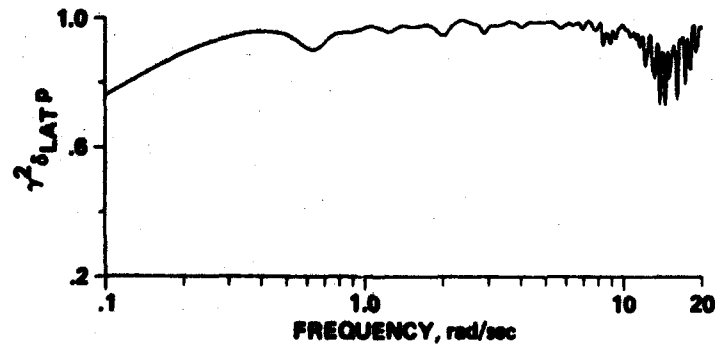


Fig. 24 Coherence function for roll rate response identification (Bell 214-ST).

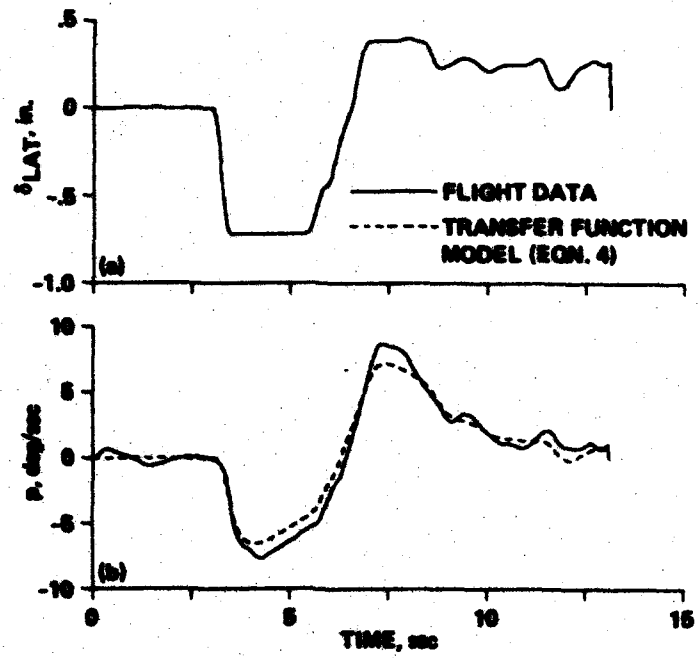


Fig. 25 Comparison of filtered aircraft response and transfer function model response to filtered-step input (Bell 214-S7): (a) lateral stick deflection, (b) roll-rate response.

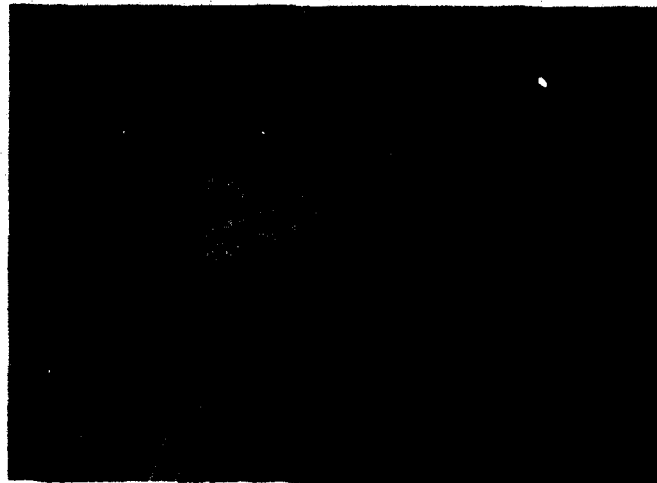


Fig. 26 CH-47B variable-stability research helicopter.

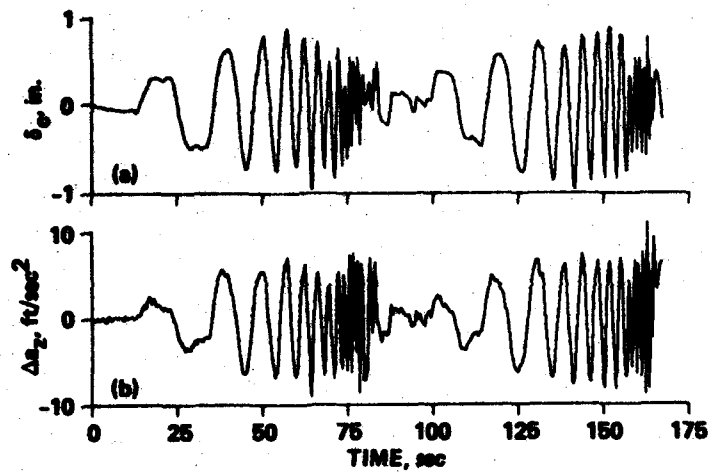


Fig. 27 Collective control input and vertical acceleration response (CH-47B flight-test data).

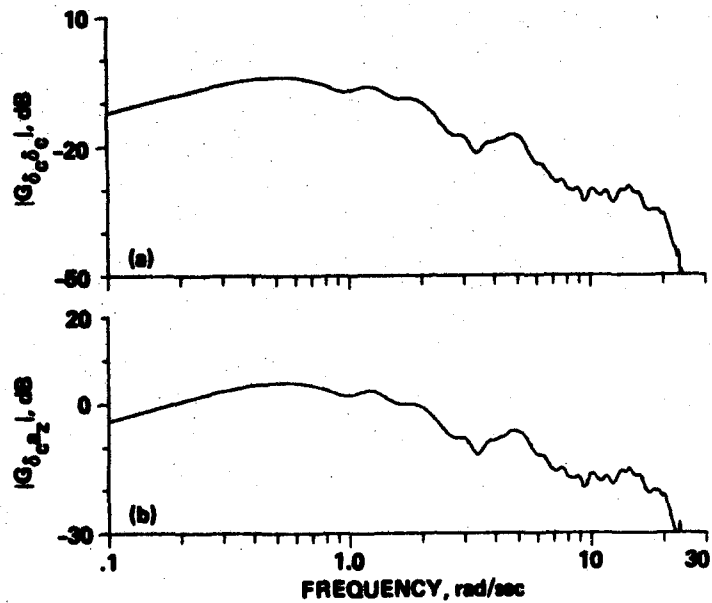


Fig. 28 Auto-spectrum of collective input and cross-spectrum of collective input and vertical acceleration response (CH-47B flight data).

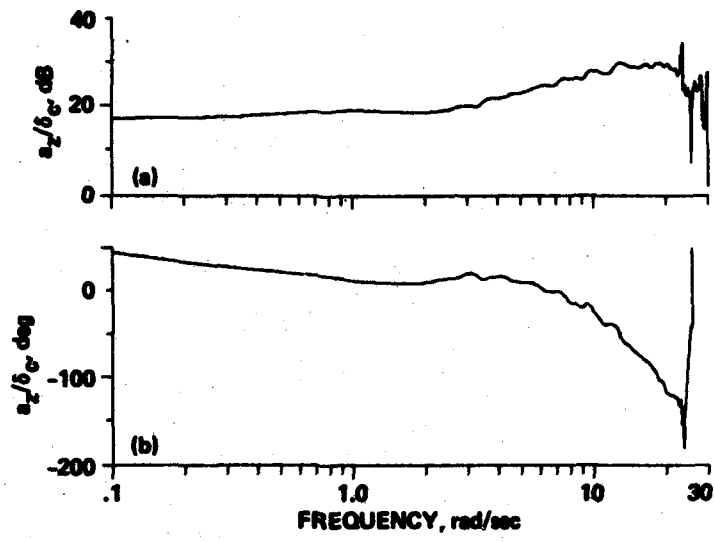


Fig. 29 Frequency responses of vertical acceleration to collective input (CH-47B flight data).

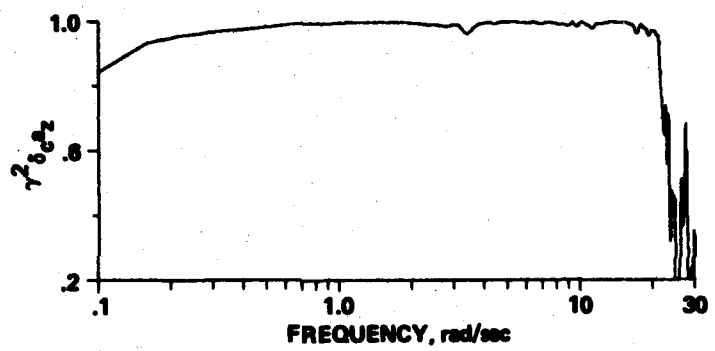


Fig. 30 Coherence function associated with transfer-function identification.

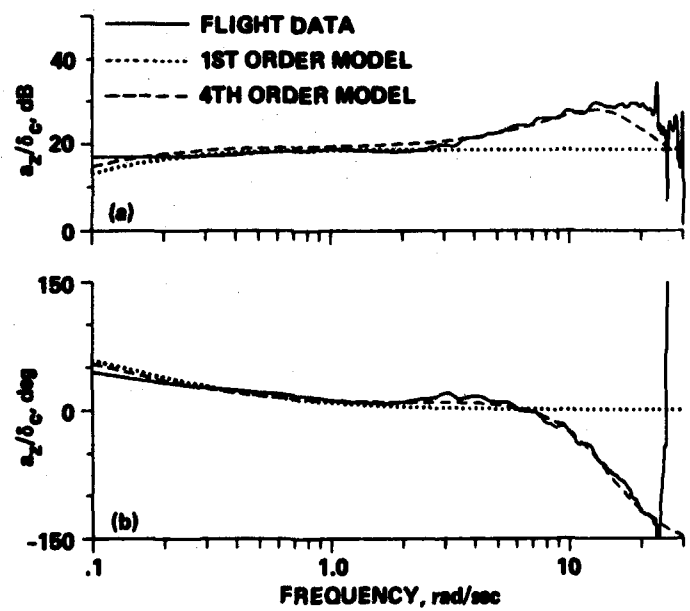


Fig. 31 Transfer-function models fit to flight extracted frequency-response data: (a) magnitude, (b) phase.

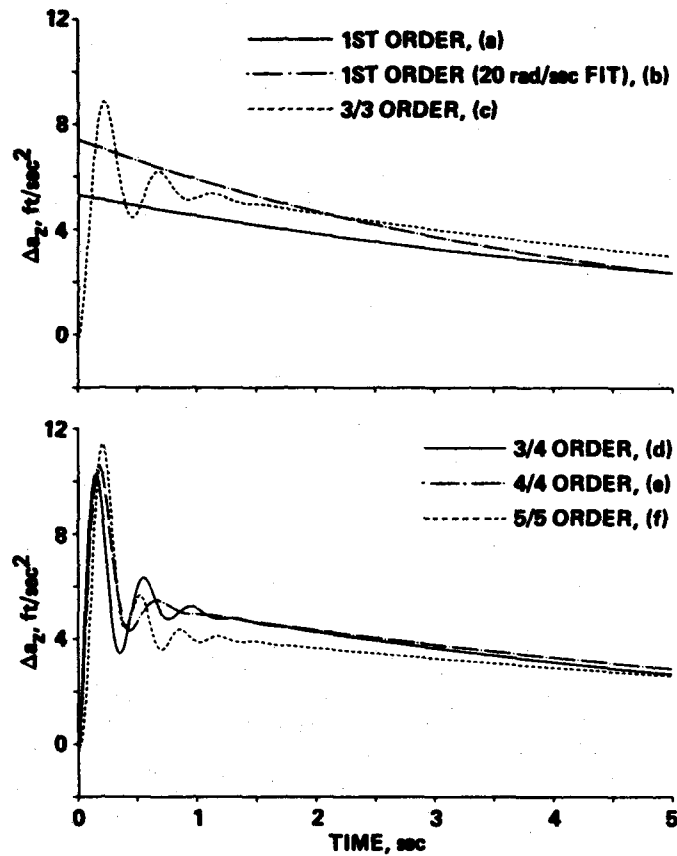


Fig. 32 Predicted  $a_z$  responses to step collective input (0.62 in.) from the six identified models.

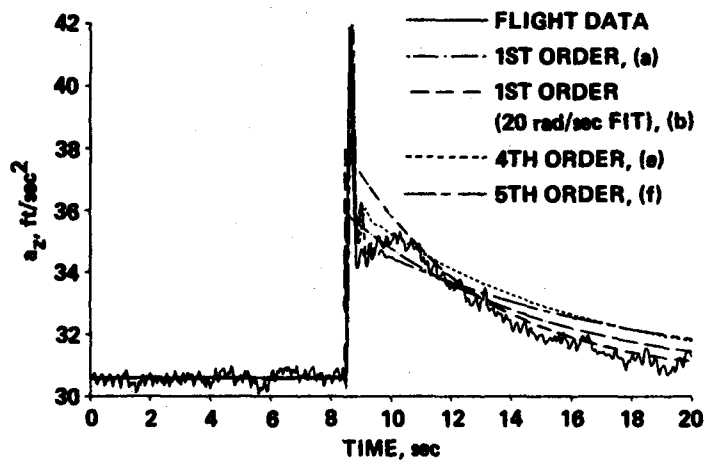


Fig. 33 Flight data, predicted responses of 1st, 4th, and 5th order models.

END

1-87

DTIC